



HAL
open science

Effects of motor tempo on frontal brain activity: An fNIRS study

Sékolène M. R. Guérin, Marion A. Vincent, Costas I. Karageorghis, Yvonne N. Delevoeye-Turrell

► **To cite this version:**

Sékolène M. R. Guérin, Marion A. Vincent, Costas I. Karageorghis, Yvonne N. Delevoeye-Turrell. Effects of motor tempo on frontal brain activity: An fNIRS study. *NeuroImage*, 2021, 230, pp.117597. 10.1016/j.neuroimage.2020.117597 . hal-03363512

HAL Id: hal-03363512

<https://hal.science/hal-03363512v1>

Submitted on 13 Feb 2023

HAL is a multi-disciplinary open access archive for the deposit and dissemination of scientific research documents, whether they are published or not. The documents may come from teaching and research institutions in France or abroad, or from public or private research centers.

L'archive ouverte pluridisciplinaire **HAL**, est destinée au dépôt et à la diffusion de documents scientifiques de niveau recherche, publiés ou non, émanant des établissements d'enseignement et de recherche français ou étrangers, des laboratoires publics ou privés.



Distributed under a Creative Commons Attribution - NonCommercial - NoDerivatives 4.0 International License


1 **Effects of Motor Tempo on Frontal Brain Activity: An *f*NIRS Study**


2 Ségolène M. R. Guérin¹, Marion A. Vincent¹, Costas I. Karageorghis², and Yvonne N.
3 Delevoeye-Turrell*¹


4 ¹Univ. Lille, UMR 9193 - SCALab - Sciences Cognitives et Sciences Affectives, F-59000
5 Lille, France

6 ²Brunel University London, Uxbridge, Middlesex, United Kingdom
7

8 **Author Note**

9 Ségolène M. R. Guérin  <https://orcid.org/0000-0003-0990-9408>

10 Marion A. Vincent  <https://orcid.org/0000-0002-1761-7491>

11 Costas I. Karageorghis  <https://orcid.org/0000-0002-9368-0759>

12 Yvonne N. Delevoeye-Turrell  <https://orcid.org/0000-0003-4034-3684>

13 The approved Stage 1 protocol is available here:

14 https://osf.io/ne6xp/?view_only=a82761c903a446608493c132329525eb. The study data
15 and materials are shared openly as part of the publication of the article
16 (https://osf.io/jw3me/?view_only=43627073ab9f4755a1225b62d05648c0). The study
17 received financial support from the I-SITE ULNE Foundation. The authors have no
18 competing financial interests to declare. The ethics committee of the University of Lille,
19 France, approved the study (#2017-8-S52).

20 Correspondence concerning this article should be addressed to Yvonne N.

21 Delevoeye-Turrell, SCALab UMR CNRS 9193, University of Lille, Rue du Barreau, BP
22 60149, 59653 Villeneuve d'Ascq Cedex. E-mail: yvonne.delevoeye@univ-lille.fr

23 **Effects of Motor Tempo on Frontal Brain Activity: An *f*NIRS Study**

24 The coding of time by the brain remains a mystery for the simple reason that
25 there are no time-specific sensory receptors. Initial studies in neuropsychology referred
26 to a normative scale depicted in the form of an internal clock. Conceptualized by
27 Treisman (1963), the internal clock is described as a pacemaker-accumulator model that
28 has become the most popular concept model to date (Droit-Volet & Wearden, 2003). It
29 is composed of three distinct stages in which temporal information about an event **is**
30 extracted, encoded, and processed. However, the internal clock metaphor was primarily
31 created to fulfill the need of a conceptual framework, and is now challenged by
32 biological and pharmacological research, which suggests that time may be embedded
33 within the neural activity of the cortex (Buhusi & Meck, 2005).

34 Since the turn of the millennium, neuroscientific studies have indicated that
35 specific brain structures may play a function in time processing; notably the cerebellum
36 and the basal ganglia, with wider networks including the supplementary motor area, the
37 prefrontal cortex, and the posterior parietal cortex (Buhusi & Meck, 2005; Ivry &
38 Spencer, 2004; Rubia & Smith, 2004). However, a major limitation in the literature is
39 the fact that most of the neuroimaging studies have focused on the perception of time,
40 while neglecting the question of motor timing (Bareš et al., 2019; Grahn & Brett, 2007;
41 Jongsma et al., 2007). Although previous findings have indicated that the brain areas
42 dedicated to time perception are similar to those devoted to time production (Rubia &
43 Smith, 2004; Schubotz et al., 2000), due care should be taken in generalizing such
44 results given that these studies were conducted by use of functional magnetic resonance
45 imaging (*f*MRI). It is extremely difficult to execute studies with motor paradigms using
46 *f*MRI, as this technology is highly sensitive to movement artifacts.

47 Over the last decade, the noninvasive imaging method of functional near-infrared
48 spectroscopy (*f*NIRS) has become the tool of choice for those investigating motor
49 paradigms (Leff et al., 2011). It makes use of the optical properties of light in order to
50 evaluate local hemodynamic responses (i.e., increase in blood flow) in a given cortical
51 area. Notably, the brain is one of the body parts in which the metabolic activity is most

52 intense (up to 20% of energy consumption of the body at rest; Attwell et al., 2010;
53 Gusnard & Raichle, 2001) and yet it possesses no reserves of energy. Hence, the brain
54 has developed a large vascular network that can perpetually support its nutritional
55 requirements. The local electrical activity of the neurons (i.e., action potential)
56 engenders an energy cost in oxygen and glucose, that is met by metabolically active
57 cells (i.e., astrocytes; Magistretti et al., 1999). This provides the resources for effective
58 cerebral activity (León-Carrión & León-Dominguez, 2012). *fNIRS* is a neuroimaging
59 technique that provides a means by which to assess such changes in brain metabolism,
60 and thus allows the researcher to infer related neural activity.

61 Near-infrared spectrum light uses the optical window in which the diffusion of
62 light through biological tissues is the greatest. It is notable that skin, tissue, and bone
63 are mostly transparent to NIR light in the optimal spectrum of 700–900 nm, while
64 oxygenated-hemoglobin (HbO₂) and deoxygenated-hemoglobin (HHb) are stronger
65 absorbers of light. Thus, differences in the absorption spectra of HHb and HbO₂ allow
66 the calculation of the relative changes in hemoglobin concentration (Hb) through the
67 use of the degree of light attenuation at multiple wavelengths Strangman et al., 2002.
68 Consequently, *fNIRS* can provide specific information on brain oxygenation (i.e.,
69 HbO₂), deoxygenation (i.e., HHb), and the total content of hemoglobin (i.e., HbT). In
70 the present study, the *fNIRS* technique was used to measure changes in oxygenation of
71 the brain tissues over the prefrontal and motor areas. This enabled a fuller
72 understanding of the relative contributions of these brain areas to motor timing.

73 The behavioral task that is most commonly used to study motor timing in
74 experimental psychology is the tapping paradigm (Repp, 2005). Early studies measured
75 the spontaneous tapping speed of the hand—referred to as the *spontaneous motor*
76 *tempo*—to further understand people’s “natural pace” (Fraisse, 1982; Fraisse et al.,
77 1954). Among the general population, this idiosyncratic tempo is subject to
78 considerable interindividual variability (Drake & Baruch, 1995; Fraisse, 1974);
79 nevertheless, spontaneous motor tempo is found to average ~2 Hz (i.e., 500-ms time
80 intervals; McAuley et al., 2006; Moelants, 2002). *fNIRS* has been used in self-paced

81 finger-tapping paradigms (Drenckhahn et al., 2015; Holper et al., 2009; Sato et al.,
82 2007; Wilson et al., 2014). Results have shown that brain hemodynamic responses
83 depend on task complexity, with complex tasks (e.g., bimanual tapping) eliciting
84 significantly larger HbO₂ changes in the premotor area and the primary motor cortex
85 than simple unimanual tapping (Holper et al., 2009). Nonetheless, few studies have used
86 fNIRS techniques to ascertain how the brain modulates the spontaneous motor tempo.

87 Humans live in a constantly changing and evolving environment. Hence, adapted
88 behaviors require individuals to be able to accelerate or decelerate the spontaneous pace
89 of their own motor actions to facilitate smooth interaction with individuals and objects
90 present in their environment (Bryant & Barrett, 2007). Such motor timing abilities are
91 commonly assessed using sensorimotor synchronization tasks. In fact, this approach
92 concerns a form of referential behavior in which an action is temporally coordinated
93 with a predictable external event, the referent (Repp, 2005, p. 969). Sensorimotor
94 synchronization tasks have shown that the ability to adapt the timing of voluntary
95 actions to environmental constraints develops with age as well as experience. For
96 example, babies are unable to alter the speed of their natural behaviors. When required
97 to synchronize self-generated actions to slow auditory stimuli, newborns and
98 2-month-old babies were reported to be unable to slow down their non-nutritive sucking
99 rate below their spontaneous motor tempo (Bobin-Bègue et al., 2006). Similar results
100 were found in 3½-year-olds during the synchronization of hand-tapping with slow
101 auditory and visual stimuli (Bobin-Bègue & Provasi, 2008). Bobin-Bègue et al. (2006)
102 suggested that the ability to slow down movements depends on motor inhibition, a
103 process that is a component of high-level cognitive functions. Thus, it would only be
104 acquired later in ontogeny and have functional impact from 8 years and beyond
105 (Williams et al., 1999).

106 If the ability to modulate motor tempo according to the environmental
107 constraints is underpinned by cognitive functions, it should involve frontal activations.
108 Following this train of thought, Kuboyama et al. (2004, 2005) reported a gradation in
109 cerebral oxygenation of the motor cortex in accord with the frequency at which a

110 finger-tapping task was performed. Larger hemodynamic responses were found for
111 maximal speed tapping compared to slower tapping conditions. However, neither of
112 these studies investigated prefrontal activations as a concomitant of the pace of motor
113 execution.

114 The main objective of the present study was to examine the cerebral oxygenation
115 of prefrontal and motor areas simultaneously during the execution of visuomotor tasks
116 performed under different time constraints. Three forms of upper-limb movement were
117 used to control for motor complexity and facilitate generalization of the findings: A
118 simple task (i.e., finger-tapping task, discrete movements with a recognizable beginning
119 and end), a task of moderate complexity (i.e., pointing task, serial
120 individual-movements linked together to constitute a whole), and a complex task (i.e.,
121 circle drawing task, continuous movements with no recognizable beginning and end;
122 Schmidt et al., 1988). These three sensorimotor synchronization tasks were administered
123 via a computer touchscreen according to three externally-paced tempi: fast pace (i.e.,
124 300 ms), natural pace (i.e., 500 ms), and slow pace (i.e., 1200 ms). A series of self-paced
125 trials (i.e., without an auditory beep) was collected at the start of the experimental
126 session in order to record each participant's spontaneous tempo. The addition of this
127 non-cued condition allowed the research team to control for the effects of auditory cues
128 with reference to brain activations during motor production at a natural pace. To
129 ensure methodological rigor, acquisition and filtering pipelines, as well as raw data, were
130 reported (Leff et al., 2011). To discriminate between physiological noise and cerebral
131 meaningful signals, the physiological data (i.e., heart and respiratory rates) were
132 recorded throughout the experimental session so that frequency bands of such signals
133 could be regressed from the *f*NIRS data. An automatic tracking of the headset was also
134 used to monitor the exact position of the optodes in reference to the cranio-cerebral
135 correlates of the NIR channels.

136 Motor timing at the spontaneous motor tempo would lead to less prefrontal (i.e.,
137 anterior and dorsolateral prefrontal cortices) and motor (i.e., premotor and primary
138 motor cortex) activation when compared to performing the motor task at either fast or

139 slow tempi (H_1). Furthermore, action production at slow tempi would lead to a
140 significantly greater increase in cerebral oxygenation over the prefrontal lobe when
141 compared to task execution at a fast tempo, for which the increase in cerebral
142 oxygenation would involve motor areas (H_2). Similar patterns of activation would be
143 observed regardless of the complexity of the motor task being undertaken (H_3).

144 **Methods**

145 **2.1 Participants**

146 Healthy adults were recruited for the present study from among the corpus of
147 University of Lille staff and students. Participants were right-handed (assessed by use of
148 the Edinburgh Handedness Inventory; Oldfield, 1971), had normal to
149 corrected-to-normal vision, and did not present motor dysfunction or
150 neurological/psychiatric disorders. A pilot test conducted on two participants confirmed
151 that both hair density and length could induce significant noise in *f*NIRS data
152 (Figure 1). Ongoing work in our laboratory is targeting potential solutions to address
153 this limitation that pertains to *f*NIRS technology. Nevertheless, for the present study,
154 only **male** participants with very short haircuts (< 1 cm) or shaven heads were included
155 to avoid hair-related issues (McIntosh et al., 2010; Pringle et al., 1999). Participants
156 were informed of the tasks to be performed and the measurements to be taken at least
157 48 hr prior to their participation. After reading an information sheet, each participant
158 was invited to provide written informed consent. At this point, demographic data were
159 collected (sex, age, and musical expertise).

160 The sample size required for the critical statistical test of each research
161 hypothesis was calculated using G*Power (3.1.9.2; see Table 1). For H_1 , H_2 , and H_3 , the
162 *f*NIRS results of Abiru et al. (2016) were used as group parameters. For H_1 and H_2 ,
163 Tukey post hoc tests were the critical statistical tests. Because a Tukey test is
164 essentially a modified *t* statistic that corrects for multiple comparisons, required sample
165 size was also computed for paired-samples *t* tests. The power analysis indicated that 15
166 participants would be required for H_1 ($d_z = .68$; $\alpha = .05$; $1-\beta = .80$), and 16
167 participants for H_2 ($d_z = .67$; $\alpha = .05$; $1-\beta = .80$). For H_3 , required sample size was

168 also computed for paired-samples t tests. The power analysis indicated that 16
169 participants would be required ($dz = .67$; $\alpha = .05$; $1-\beta = .80$). Accordingly, a sample of
170 16 participants was recruited.

171 The small telescopes approach was used to determine the smallest effect size of
172 interest (SESOI; i.e., the difference that is considered too small to be meaningful;
173 Simonsohn, 2015) for each hypothesis. Accordingly, the SESOI was set to the effect size
174 that an earlier study would have had 33% power to detect (Lakens et al., 2018). As
175 previously, the f NIRS results of Abiru et al. (2016) were used for H_1 , H_2 , and H_3 . The
176 SESOI for each hypothesis is reported in Table 1.

177 **2.2. Experimental Procedure and Tasks**

178 *2.2.1 Experimental Procedure*

179 Each participant was administered three visuomotor tasks via a touchscreen on
180 which he used his right index finger, with a closed fist. An f NIRS headset was worn by
181 the participant throughout the session. The touchscreen (1915L Elo Touch 19"; Elo
182 Touch Solutions Inc.; Milpitas, California, CA) was placed on a table in front of the
183 participant with the screen oriented at 45° . The participant was seated on a stool,
184 suitably adjusted to her/his height to minimize lower-limb muscular fatigue (assessed
185 by use of the rating-of-fatigue scale; Micklewright et al., 2017) and avoid any extraneous
186 movements during task performance. The stool was fixed in such a way that horizontal
187 rotational movement would be possible. The experimental session took place in a quiet,
188 windowless room that was dimly lit. The lighting is of particular importance given that
189 bright light can affect f NIRS signals (Shadgan et al., 2010). The f NIRS system
190 (FOIRE-3000/16; Shimadzu, Kyoto, Japan) was placed behind the participant to limit
191 distraction and facilitate the management of the cables. This setup also provided a
192 means by which to minimize the weight of cables on the participant's neck. To verify
193 that this was effective, a self-rated pain scale of was administered. The scale was
194 attached to a 9-point Likert scale, ranging from 1 (*no pain*) to 9 (*unbearable pain*). The
195 participant was required to indicate the degree of pain that he was experiencing in
196 regard to the weight of optodes on the head and neck. This pain scale was presented at

197 the beginning of each block of trials as well as at the end of the experiment, for an
198 overall evaluation of the participant's experience.

199 *2.2.2 Task Description*

200 A total of three visuomotor tasks were administered in a counterbalanced order
201 across participants. In the finger-tapping task, the participant was required to tap on a
202 single visual target (dot of 10-mm diameter) located in the center of the touchscreen
203 (Figure 2, left panel). In the pointing task, six targets (dots of 10-mm diameter)
204 positioned around an invisible circle of 100 mm radius were displayed on the screen.
205 The participant was asked to tap each target, one after the other (Figure 2, middle
206 panel). In the drawing task, six targets of a similar nature linked together to form a
207 100-mm circle were displayed on the screen (Figure 2, right panel). The participant was
208 required to trace the circle and, in so doing, produce a regular and continuous arm
209 movement. In both the pointing and the drawing tasks, the participant was instructed
210 to start with the finger above the top-right target and move counterclockwise. The
211 participant was instructed to maintain accuracy in both temporal and spatial facets of
212 the skill, but to favor temporal accuracy in case the task became too challenging for
213 both to be maintained.

214 The participant performed the tapping, pointing, and drawing tasks at three
215 predefined tempi that were set by an auditory metronome. The beeps of the metronome
216 had a duration of 80 ms and a sound frequency of 294 Hz. The beeps were generated
217 using Matlab 7.11.0 R2010 software (Mathworks Inc.; Natick, Massachusetts, MA).

218 The three tempi used in the study were 300 ms (for the fast-tempo trials), 500
219 ms (for the natural-tempo trials), and 1200 ms (for the slow-tempo trials). For the fast-
220 and slow-tempo trials, this enabled the participant to depart from her/his spontaneous
221 motor tempo but remain within the possible sensorimotor synchronization zone
222 (between 180 ms and 1800 ms, Keele et al., 1985; Mates et al., 1994). These metronome
223 tempi were played to the participant via two Creative SBS 250 desk speakers (Creative
224 Technology; Singapore) positioned either side of the screen.

225 **2.2.3 Experimental Design**

226 The experiment was predicated on a block design procedure, characterized by
227 alternating periods of activity and respite to facilitate the acquisition of reliable *f*NIRS
228 signals (Gervain et al., 2011). It has been shown that the best *f*NIRS signal is obtained
229 with a resting period of 30 s prior to stimulation (Obrig et al., 1997). Accordingly, each
230 60-s trial was preceded by a rest period of 30 s to allow the hemodynamic indices to
231 return to their baseline levels and to optimize the quality of the hemodynamic responses
232 to time-locked body movements.

233 The participant performed a series of 12 blocks, for a total of 36 trials. In a first
234 series, the participant performed the three visuomotor tasks in a randomized order at a
235 self-paced spontaneous tempo (i.e., executed at a regular and most natural pace). In a
236 second series, he performed the three visuomotor tasks while synchronizing their
237 movements to the metronome. Three blocks of trials were recorded for each task, with
238 the slower, natural, and faster conditions administered in a random order.

239 Throughout the session, the participant was instructed to leave his left arm
240 hanging by their side in a relaxed manner. The participant was also informed not to
241 speak and to avoid extraneous movements during each *f*NIRS trial. The self-paced trials
242 were systematically administered before the externally-paced trials to avoid
243 cross-contamination (Bove et al., 2009). The total duration of the experimental test
244 period was ~100 min.

245 **2.3 Data Acquisition and Preprocessing Analyses**

246 **2.3.1 Behavioral Data Acquisition and Preprocessing**

247 In the tapping and pointing tasks, inter-response intervals (IRIs) were measured
248 as the time interval between the onset of successive taps. In the drawing task, radiuses
249 from the center of the circle to each target were computed first. Taps were defined as
250 the locus that intersected the participant's finger and each radius. Before conducting
251 the main analyses, the time series were checked in order to detect and remove the IRIs
252 greater than twice the ISI of the given block of trials. These trials were referred to as
253 "temporal omissions" and were not included in the statistical analyses.

254 An IRI error (IRI_{error}) was computed as the percentage of absolute difference
255 between an IRI and its reference ISI for a given time interval t (Equation 1).

$$IRI_{\text{error}(t)} = (|IRI_t - ISI|) / ISI \times 100 \quad (1)$$

256 The mean IRI_{error} measurement within a trial indicated the accuracy of time interval
257 production (i.e., behavioral tempo-accuracy; Repp, 2005).

258 For each time interval t , a spatial error was computed (pixels), as the difference
259 between the center of the visual target and the location of the participant's forefinger.
260 The mean pointing error within a trial was used as an indicator of behavioral-spatial
261 accuracy (Dione & Delevoeye-Turrell, 2015).

262 **2.3.2 fNIRS Data Acquisition**

263 Data were collected using a continuous-wave fNIRS system operating at three
264 near-infrared wavelengths (780 nm, 805 nm, and 830 nm) and monitored by the
265 associated LabNIRS software. This fNIRS system offers 32 optodes divided into 16 light
266 sources (multicomponent glass bundle fibers) and 16 detectors (multi-alkali
267 photomultipliers detectors). The sampling frequency was set at 2.27 Hz (i.e., temporal
268 resolution of 440 ms).

269 The brain regions of interest were the prefrontal cortex (anterior and dorsolateral
270 prefrontal cortices; Brodmann's areas 9 and 10) and motor cortex (premotor and
271 primary motor cortices; Brodmann's areas 4 and 6; Homan et al., 1987; Okamoto et al.,
272 2004). Thus, a 45-channel (28 optodes, 45 source-detector couples) configuration was
273 applied in order to cover these cortices over both brain hemispheres (Figure 3). One
274 additional channel was applied to the occipital cortex (Brodmann's area 18) as a means
275 of providing "negative control" (i.e., control an area of the brain not expected to be
276 influenced by the experimental manipulations). The optodes were attached to a
277 32-optode headset with a 3-cm source-detector distance, giving a depth of analysis from
278 0.5–2.0 cm. The headset was placed on each participant's head in accord with the
279 International 10–20 system guidelines for standard electrode positions (Jasper, 1958). As
280 a result, the Cz optode was located at the midway point between the nasion and inion.

System calibration was performed through an automatic adjustment using LabNIRS to adapt the internal parameters of the *f*NIRS device (e.g., gain, amount of light to emit) to the head morphology and the hair-type characteristics of each participant. Differences in the absorption of HbO₂ and HHb provided the means to measure the differences in the hemoglobin concentration (μmol/L). These differences were computed in real time using Equation 2 and 3 (generated by LabNIRS from the modified Beer-Lambert law; Baker et al., 2014):

$$\text{HbO}_2 = (-1.4887) \times \text{Abs}[780\text{nm}] + 0.5970 \times \text{Abs}[805\text{nm}] + 1.4847 \times \text{Abs}[830\text{nm}] \quad (2)$$

$$\text{HHb} = 1.8545 \times \text{Abs}[780\text{nm}] + (-0.2394) \times \text{Abs}[805\text{nm}] + (-1.0947) \times \text{Abs}[830\text{nm}] \quad (3)$$

281 The total hemoglobin (HbT) will then be established through a summation of HbO₂
282 and HHb (Equation 4):

$$\text{HbT} = \text{HbO}_2 + \text{HHb} \quad (4)$$

283 **2.3.3 Preprocessing of *f*NIRS Data**

284 Data (HHb, HbO₂, and HbT) were first filtered to eliminate mechanical artifacts
285 (quick baseline shifts of the signal waveform characterized by sharp and steep edges)
286 and physiological noise (heart and respiratory rates). This enabled the research team to
287 keep only the physiological hemodynamic signals X (HHb, HbO₂, and HbT), which
288 show slow variations over time (Pinti et al., 2019). The precise preprocessing pipeline
289 was defined in accord with the shape of the data, as there is presently no consensus in
290 the *f*NIRS literature regarding filtering methods (Pinti et al., 2019).

291 For each trial i , a baseline $B_{X,i}$ and a plateau $P_{X,i}$ were defined as the mean
292 values of X upon a 5-s time window starting 10 s before the trial onset and upon the
293 last 5 s of the trial, respectively (for similar calculations, see Mandrick, 2013). Then, the
294 variations $\Delta_{X,i}$ of a trial were given relative to its baseline (i.e., by subtracting $B_{X,i}$ to
295 $P_{X,i}$), to be free from possible offsets across trials and linear trends of the signal over
296 time. The mean $\bar{\Delta}_{X,n}$ was computed over each block n , for each channel, in each
297 condition (for similar calculations, see Derosière et al., 2014; Mandrick et al., 2013).
298 Finally, the mean variations in HbO₂, HHb, and HbT were given for two channel
299 clusters defined according to the two regions of interest: $\bar{\Delta}_{X, \text{prefrontal}}$ and $\bar{\Delta}_{X, \text{motor}}$.

300 **2.3.4 Controlling for Noisy Signals**

301 Data contamination caused by movement and physiological artifacts in *f*NIRS is
302 an important consideration with regard to reaping the full potential of the technique for
303 real-life applications (Jahani et al., 2018). In the present study, we applied tracking
304 methods to identify sources of noisy data. The synchronization of the different systems
305 was controlled by means of Matlab algorithms. The central command computer
306 controlled for motor tasks; it sent triggers to the other apparatus—including the *f*NIRS
307 system—to segment the times of onsets and offsets in an automated manner. A similar
308 triggering system was used in our previous studies (e.g., Blampain et al., 2018), which
309 revealed a synchronization error of ~35 ms. Visual tags were used to identify the
310 beginning and end of each trial, with specific tags for each trial type.

311 **2.3.4.1 Cardiorespiratory Monitoring**

312 By use of the Fourier transform method, both heart and respiratory rates can be
313 identified in the *f*NIRS frequency spectrum. The ability to identify these two frequency
314 components serves to ensure the validity of *f*NIRS measures. In terms of frequency, the
315 neurophysiological detail in the *f*NIRS signals is lower than that of both heart and
316 respiratory rates (~2 Hz and ~0.3 Hz, respectively; Pinti et al., 2019). Thus, these
317 physiological components were filtered out, which restricted any potential
318 contamination from the raw *f*NIRS signal.

319 Cardiorespiratory monitoring was done using the MP150 Biopac system (Biopac
320 Systems, Goleta, CA), complemented with two dedicated add-on wearable devices. To
321 avoid recording movement artifacts, heart rate (HR) data (Hz) were captured by use of
322 an ECG Bionomadix module (wireless transmitter and RPEC-R amplifier) and low-pass
323 filtered to 1 Hz. Two disposable patch electrodes were placed on the participant's right
324 and left clavicles. Respiration rate (Hz) was recorded using the TSD201 respiratory
325 effort transducer, which was wired to the RSP100C amplifier. This respiratory belt was
326 placed around the chest wall, at the level of the sternum. Sampling frequency was set to
327 250 Hz. Data acquisition was **facilitated by** the AcqKnowledge software that is included
328 in the MP system.

329 2.3.4.2 Headset Position Tracker

330 Data were collected using three Oqus 5+ cameras (Qualisys MoCap, Göteborg,
 331 Sweden) to control for any shift in the headset. The spatial positions were measured in
 332 real time using three spherical passive markers taped to the participant's right temple
 333 and headset (with the use of one and two markers, respectively). The distance between
 334 the temple marker and each of the two headset markers was computed (in cm) based on
 335 Cartesian coordinates (i.e., x , y , and z). The Real-Time Motion Capture (RTMocap)
 336 Matlab toolbox (Lewkowicz & Delevoeye-Turrell, 2016) was used to interpolate any
 337 missing data. The spatial accuracy of the system is 0.5 mm for each dimension of 3D
 338 space.

339 To verify the occurrence of a f NIRS helmet shift, a deformation calculation of
 340 the area of the planar triangle connecting the 3D markers was used. This was referred
 341 to as the *mesh area*. Notably, if the 3D markers remain in the same place with respect
 342 to each other, the mesh area remains constant. On the other hand, if the two markers of
 343 the headset move relative to the reference marker (i.e., temple marker), the mesh area is
 344 modified.

345 The mesh area between the three markers M_i , with $i \in \{0; 1; 2\}$, at a given
 346 moment in time $t \in [1; d]$, with d defined as the acquisition duration, was computed
 347 using a scalar product (Equation 5), equal to twice the mesh area.

$$\overrightarrow{M_0M_1}(t) \cdot \overrightarrow{M_0M_2}(t) = \begin{pmatrix} x_1(t) - x_0(t) \\ y_1(t) - y_0(t) \\ z_1(t) - z_0(t) \end{pmatrix} \cdot \begin{pmatrix} x_2(t) - x_0(t) \\ y_2(t) - y_0(t) \\ z_2(t) - z_0(t) \end{pmatrix} \quad (5)$$

348 If $\overrightarrow{M_0M_1} \cdot \overrightarrow{M_0M_2}$ remained constant over time with an acceptable error threshold,
 349 an absence of deformation of the mesh was considered and indicative of an absence of
 350 headset shift. In the present study, the error threshold ϵ was set to 10 mm, which
 351 corresponds to the degree of spatial resolution of the f NIRS optical imaging technique
 352 (Quaresima & Ferrari, 2016). The variation Δ_{mesh} of the $\overrightarrow{M_0M_1} \cdot \overrightarrow{M_0M_2}$ value was
 353 computed. If this value exceeded 15%, which corresponds with ϵ , the participant's data
 354 from that block of trials as well as from subsequent blocks were removed for the

355 purposes of statistical analysis, as it was difficult to determine the exact sources of the
356 recorded hemodynamic signals.

357 **2.4 Statistical Analyses**

358 ***2.4.1 Data Eligible for Analysis***

359 HbT reflects the overall changes in corpuscular blood volume of the sampling
360 volume. Because HbT is a summation of HbO₂ and HHb changes (see Equation 4), it
361 was not statistically analyzed. The behavioral data were analyzed and reported in a
362 supplementary online file. HHb and HbO₂ data were analyzed only from those blocks of
363 trials characterized by (a) at least 70% level of behavioral accuracy, and (b) an absence
364 of headset shift. A participant's entire data set was removed if > 25% of his data were
365 ineligible and any excluded participants were replaced.

366 Given that an absence of cerebral activation can be informative, both activated
367 and non-activated channels were taken into consideration. In addition, the ratio of
368 activated to non-activated channels (i.e., if $B_{X,i}$ and $P_{X,i}$ are significantly different) was
369 reported for each trial. Only HbO₂ data were used to support or refute hypotheses.
370 However, HHb data were also statistically analyzed to improve specificity of *f*NIRS
371 signals, as recommended in the *f*NIRS literature (e.g., Leff et al., 2011; Tachtsidis &
372 Scholkmann, 2016). The alpha level was set at $p < .05$ for all statistical analyses.

373 ***2.4.2 Analyses Undertaken***

374 **2.4.2.1 Classic Null-Hypothesis Significance Tests**

375 The dependent variables, $\bar{\Delta}_{\text{HbO}_2}$ and $\bar{\Delta}_{\text{HHb}}$ for each of the two regions of interest
376 were analyzed. To examine H_1 and H_2 , a oneway RM MANOVA (Externally-Paced
377 Tempo [300 ms, 500 ms, 1200 ms]) was applied. Normality was checked using the
378 Shapiro–Wilk test; if violated, the data were normalized using a transformation that
379 was contingent on data distribution curves (e.g., log10). Where Mauchly's tests
380 indicated violations of the sphericity assumption, Greenhouse–Geisser corrections were
381 applied. Tukey post hoc tests were used where necessary (see Table 1).

382 **2.4.2.2 Equivalence Tests**

383 It is not acceptable to use nonsignificance of the interaction term from an
384 ANOVA to claim the absence of an interaction effect (Cribbie et al., 2016).
385 Consequently, to confirm that similar effects of externally-paced tempo were observed
386 regardless of the task complexity (H_3), two one-sided tests (TOSTs) were used (Lakens
387 et al., 2018). In this procedure—referred to as *equivalence testing*—the SESOI is used to
388 test whether an effect is sufficiently close to zero to reject the presence of a meaningful
389 difference (Harms & Lakens, 2018, p. 385). The results of both t tests needed to reach
390 significance in order for equivalence to be claimed. To date, the TOST procedure has
391 only been used in a oneway ANOVA design (Campbell & Lakens, 2020), and has yet to
392 be extended to interaction effects. Accordingly, TOST were computed on the *change*
393 *score* (i.e., difference between the 300-ms and 1200-ms tempo trials) between (a) the
394 simple and moderate tasks, (b) the simple and complex tasks, and (c) the moderate and
395 complex tasks. TOSTs were computed using the TOSTER R package for
396 paired-samples t tests (Lakens, 2017).

397 **2.4.3 Outcome-neutral validation tests**

398 The f NIRS technique is rather new in the field of human brain sciences and so
399 defining a positive control provides many challenges. Consequently, a negative control
400 condition was included by placing an additional channel over the occipital brain region
401 (Brodmann’s area 18). This region is involved primarily in visual perception and so its
402 activation should remain fairly consistent across pacing conditions and motor tasks.
403 Accordingly, TOSTs (Lakens et al., 2018) were computed for paired-samples t tests
404 between the baseline $B_{X,occipital}$ and the plateau $P_{X,occipital}$ for each block of trials.
405 Statistically nonsignificant differences provided a means by which to confirm that
406 observed prefrontal and motor activations are related to the modulation of motor
407 tempo. If differences were detected over the occipital brain region, the delta activation
408 was removed from all other delta values.

409

3. Results

3.1 Behavioral Data

3.1.1 Time-Interval Accuracy

The RM ANOVA showed a significant main effect of motor tempo, $F(2, 24) = 6.88$, $p = .004$, $\eta_p^2 = .36$, with more IRI_{error} in the 300 ms ISI ($M = 10.79$, $SD = 3.39$) than in the 500 ms ($M = 8.54$, $SD = 2.84$) and 1200 ms ISI conditions ($M = 8.23$, $SD = 2.74$; Figure 4). The main effect of task complexity was also significant, $F(2, 24) = 77.86$, $p < .001$, $\eta_p^2 = .87$, with a smaller IRI_{error} in the simple ($M = 4.51$, $SD = 1.62$) and moderate tasks ($M = 5.89$, $SD = 1.59$) compared to the complex task ($M = 17.17$, $SD = 5.75$). The Motor Tempo \times Task Complexity interaction was nonsignificant ($p = 0.117$). Overall, the results indicated that participants made more timing errors under a fast externally-paced tempo and when the task was complex.

3.1.2 Spatial Accuracy

The RM ANOVA showed a significant main effect of motor tempo, $F(2, 24) = 20.38$, $p < .001$, $\eta_p^2 = .63$, with the spatial errors decreasing from the 300 ms ISI ($M = 42.75$, $SD = 13.04$) to the 1200 ms ISI ($M = 24.58$, $SD = 11.86$). The main effect of task complexity was also significant, $F(2, 24) = 78.88$, $p < .001$, $\eta_p^2 = .87$, with fewer spatial errors in the simple task ($M = 9.56$, $SD = 2.61$) than in the complex one ($M = 22.34$, $SD = 14.98$), and in the complex than in the moderate task ($M = 100.73$, $SD = 16.53$). The Motor Tempo \times Task Complexity interaction was significant, $F(4, 48) = 8.54$, $p = .001$, $\eta_p^2 = .42$. This indicated that spatial errors were smaller in the simple task than in the complex one in the 300 ms ($p < .001$) and the 500 ms ISI conditions ($p < .001$); however, the spatial errors were similar in the simple and complex tasks in the 1200 ms ISI condition (Figure 4). Overall, the results showed that participants made more spatial errors when required to move through space quickly.

3.2 Headset Position Tracker

The absolute variation Δ_{mesh} did not exceed the 15% threshold for any of our participants ($M = 0.91$, $SD = 0.87$). The maximum percentage change observed was

437 3.13%. Overall, the data confirmed the absence of an *f*NIRS helmet shift, meaning that
438 the 3D markers held the same relative positions throughout the experimental trials.

439 **3.3 *f*NIRS Data**

440 **3.3.1 Preprocessing**

441 Given that our *f*NIRS system does not provide access to raw intensities,
442 preprocessing was performed directly on Δ_{HbO_2} and Δ_{HHb} concentrations. This was
443 achieved using Matlab, with both personal code and algorithm adapted from the
444 Matlab-based toolbox Homer2 (Massachusetts General Hospital, Boston, MA, USA).
445 The preprocessing steps are detailed in Figure 5.

446 The *f*NIRS literature details several filtering methods (Herold et al., 2018; Hocke
447 et al., 2018; Pinti et al., 2019) and a hybrid filtering of the *f*NIRS time-series was
448 applied in the present study (cf. Jahani et al., 2018). First, the wavelet-based method
449 was used to perform motion-artefact correction, as it appeared to apply particularly
450 well to our dataset, and has been shown to be relatively efficient (Hocke et al., 2018).
451 Second, *f*NIRS data were bandpass filtered to remove physiological noise that was
452 concomitant to the task-induced hemodynamic activity.

453 **3.3.1.1 Channel Exclusion Criterion**

454 The first mandatory step was to control for the optical-coupling quality of the
455 acquired *f*NIRS data (Orihuela-Espina et al., 2010; Pinti et al., 2019; Scholkmann et al.,
456 2017). Optical coupling is characterized by the presence of heart-beat oscillations within
457 the *f*NIRS signals. A frequency inspection of the raw *f*NIRS time series enabled the
458 exclusion of channels with a poor optical coupling (i.e., an absence of HR in the power
459 spectrum of *f*NIRS signals). Only Δ_{HbO_2} raw data were analyzed, as HbO₂ is more
460 sensitive to cardiac oscillation than HHb (Pinti et al., 2019). A two-step process was
461 used to check the 45 channels for each participant: First, applying power-spectrum
462 density (PSD; i.e., frequency domain) to the raw data, the frequency corresponding to
463 maximal peak in the 50–160 beat-per-minute (bpm) range was detected. Second, to
464 guarantee that the identified frequency was indeed the HR frequency, it was compared

465 to the HR measurements provided by the Biopac system, with a tolerance threshold of 7
466 bpm.

467 Following the aforementioned steps, three participants were excluded due to an
468 absence of heart beat oscillations in the *f*NIRS signal across all channels pertaining to
469 at least one region of interest. In addition, the channels for which we failed to identify
470 cardiac-frequency component for all participants were excluded from subsequent
471 statistical analyses. Overall, 34.8% of channels were rejected on this basis. Examples of
472 both acceptable and excluded channels are shown in Figure 6.

473 **3.3.1.2 Motion Correction: Wavelet Filtering**

474 *f*NIRS signals recorded during body movements are prone to motion artefacts.
475 Accordingly, motion correction was performed to remove motion-induced sharp and fast
476 skips from the raw *f*NIRS time series (see Figure 7). To this end, the wavelet-based
477 smoothing method described by Molavi and Dumont (2012) and implemented in
478 Homer2 (`hmrMotionCorrect_Wavelet` function, interquartile-range [*iqr*] = 1.5) was
479 adapted to process concentrations rather than of optical densities. The motion-corrected
480 data were visually inspected to ensure that the selected *iqr* value was well suited to the
481 present dataset.

482 **3.3.1.3 Bandpass Filtering of Physiological Noise**

483 Hemodynamic responses elicited by a cognitive process are jeopardized by
484 physiological processes that are not directly linked to the task being undertaken
485 (Scholkmann et al., 2014; Tachtsidis et al., 2004). To minimize the effects of
486 spontaneous hemodynamic activity—HR (~1 Hz), breathing rate (~0.3 Hz), Mayer
487 waves (i.e., arterial pressure oscillations; ~0.1 Hz), and very low frequency oscillations
488 (VLF, < 0.04 Hz)—motion-corrected *f*NIRS signals were bandpass filtered.

489 A third-order Butterworth filter was applied to extract relevant frequencies
490 (Figure 7) The high cut-off frequency (lowpass) was set to 0.09 Hz to reject both
491 cardiac and breathing rates and parts of Mayer oscillations. The highpass was set at
492 0.003 Hz to preserve the stimulation protocol frequency ($1 / (\text{task} + \text{rest}) = 0.01$ Hz)
493 without attenuation (0 dB flat frequency band of the filter). The 2nd and 3rd harmonics

494 that contained important information were also preserved (Pinti et al., 2019). Figure 7
495 summarizes the steps taken in the hybrid filtering process.

496 **3.3.2 Outcome-Neutral Validation Tests**

497 The TOST procedure (SESOI = 0.8) showed that both t tests were significant,
498 $t_{\text{upper}}(15) = -4.48$, $p < .001$, $t_{\text{lower}}(15) = 1.92$, $p = .037$. Thus, equivalence was
499 established, confirming that occipital activations remained similar across tempo
500 conditions and levels of task complexity.

501 **3.3.3 Oxygenated Hemoglobin**

502 To detect non-activated channels, $\bar{\Delta}_{\text{HbO}_2}$ was tested against zero by means of a
503 one-sided t test within each of the 45 channels. To account for multiple comparisons,
504 Bonferroni corrections were applied ($.05 \div 45$; $\alpha = .001$). Results showed that all $\bar{\Delta}_{\text{HbO}_2}$
505 were significantly different from zero. Collectively, the results indicate that 100% of the
506 channels were activated.

507 **3.3.3.1 Motor Channels**

508 The RM ANOVA showed a significant main effect of motor tempo, $F(2, 30) =$
509 5.77 , $p = .007$, $\eta_p^2 = .28$, with a smaller $\bar{\Delta}_{\text{HbO}_2}$ in the 1200 ms ISI ($M = 1.85$, $SD =$
510 6.52) than in the 300 ms ISI ($M = 4.94$, $SD = 7.60$, $d_z = 0.43$) and the 500 ms ISI
511 conditions ($M = 4.23$, $SD = 7.26$, $d_z = 0.34$; Figure 8). Note that the effect size of both
512 contrasts was larger than the required SESOI (see Table 1), which indicated that the
513 effects were sufficiently strong to be considered meaningful.

514 The TOST procedure (SESOI = 0.62; Miyai et al., 2001) computed on the
515 change score between the simple and moderate tasks showed that both t tests were
516 significant, $t_{\text{upper}}(15) = -2.97$, $p = .005$, $t_{\text{lower}}(15) = 1.97$, $p = .034$. However, neither of
517 the TOST procedures computed on the change score between (a) the simple and
518 complex tasks ($p_{\text{upper}} = .003$, $p_{\text{lower}} = .159$), and (b) the moderate and complex tasks
519 ($p_{\text{upper}} = .002$, $p_{\text{lower}} = .183$) reached significance. Overall, the results confirmed similar
520 effects of motor tempo across the simple and moderate tasks over the motor areas (see
521 Table 2).

522 3.3.3.2 Prefrontal Channels

523 The RM ANOVA showed a significant main effect of motor tempo, $F(2, 30) =$
524 3.93 , $p = .030$, $\eta_p^2 = .21$, with a larger $\bar{\Delta}_{\text{HbO}_2}$ in the 500 ms ISI ($M = 3.75$, $SD = 6.51$)
525 than in the 1200 ms condition ($M = 1.06$, $SD = 5.52$, $d_z = 0.44$; Figure 8). Note that
526 the effect size of the contrast was larger than the required SESOI, which indicated that
527 the effect was sufficiently strong to be considered meaningful.

528 The TOST procedure (SESOI = 0.62) computed on the change score between
529 the simple and moderate tasks showed that both t tests were significant, $t_{\text{upper}}(15) =$
530 -2.56 , $p = .011$, $t_{\text{lower}}(15) = 2.38$, $p = .015$. However, neither of the TOST procedures
531 computed on the change score between (a) the simple and complex tasks ($p_{\text{upper}} = .007$,
532 $p_{\text{lower}} = .072$), and (b) the moderate and complex tasks ($p_{\text{upper}} = .007$, $p_{\text{lower}} = .069$)
533 were significant. Overall, these results indicated similar effects of motor tempo across
534 the simple and moderate complexity tasks over the prefrontal areas (see Table 2).

535 3.3.4 Deoxygenated Hemoglobin

536 3.3.4.1 Motor Channels

537 The RM ANOVA ran on the $\bar{\Delta}_{\text{HHb}}$ was nonsignificant ($p = .749$). The TOST
538 procedure (SESOI = 0.62) computed on the change score between the simple and
539 moderate tasks showed that both t tests were significant, $t_{\text{upper}}(15) = -2.20$, $p = .022$,
540 $t_{\text{lower}}(15) = 2.75$, $p = .008$. However, neither of the TOST procedures computed on the
541 change score between (a) the simple and complex tasks ($p_{\text{upper}} = .008$, $p_{\text{lower}} = .062$),
542 and (b) the moderate and complex tasks ($p_{\text{upper}} = .007$, $p_{\text{lower}} = .073$) were significant.
543 Overall, these results indicated similar effects of motor tempo across the simple and
544 moderate complexity tasks over the motor areas (see Table 2).

545 3.3.4.2 Prefrontal Channels

546 The RM ANOVA performed on the $\bar{\Delta}_{\text{HHb}}$ was nonsignificant ($p = .529$). The
547 TOST procedure (SESOI = 0.62) computed on the change score between the simple
548 and moderate tasks showed that both t tests were significant, $t_{\text{upper}}(15) = -2.92$, $p =$
549 $.005$, $t_{\text{lower}}(15) = 2.03$, $p = .030$. The TOST procedure computed on the change score
550 between the moderate and complex tasks showed that both t tests were significant,

551 $t_{\text{upper}}(15) = -2.63$, $p = .011$, $t_{\text{lower}}(15) = 1.82$, $p = .047$. However, the TOST procedure
552 computed for the change score between the simple and complex tasks was nonsignificant
553 ($p_{\text{upper}} = .007$, $p_{\text{lower}} = .071$). Overall, these results indicated similar effects of motor
554 tempo over the prefrontal area across the simple and moderate complexity tasks, and in
555 the moderate and complex tasks (see Table 2).

556 3.4 Exploratory Analyses

557 Through visual inspection, we noticed that HbO_2 began to increase just prior to
558 initiation of the task (see Figure 8). It is notable that the epoch used to compute
559 $B_{\text{HbO}_2,i}$ (i.e., from 5 s to 10 s before the trial onset) coincided with when HbO_2 had
560 already started to increase. To make $B_{\text{HbO}_2,i}$ more representative of the baseline level,
561 additional analyses were applied for which $B_{\text{HbO}_2,i}$ was taken from 20 s to 10 s prior to
562 trial onset. These findings are presented in the paragraphs that follow.

563 The RM ANOVA performed on the motor channels showed a significant main
564 effect of motor tempo, $F(2, 30) = 7.04$, $p = .003$, $\eta_p^2 = .32$, with a smaller $\bar{\Delta}_{\text{HbO}_2}$ in the
565 1200 ms ($M = 3.06$, $SD = 5.21$) than in the 300 ms ISI ($M = 6.74$, $SD = 6.65$, $d_z =$
566 0.59) and the 500 ms ISI conditions ($M = 5.94$, $SD = 6.05$, $d_z = 0.50$). Note that the
567 effect size of both contrasts was larger than the required SESOI, which indicated that
568 the effects were strong enough to be considered meaningful. None of the TOST
569 procedures computed on the change score between (a) the simple and moderate tasks
570 ($p_{\text{upper}} = .001$, $p_{\text{lower}} = .093$), (b) the simple and complex tasks ($p_{\text{upper}} = .005$, $p_{\text{lower}} =$
571 $.097$), and (c) the moderate and complex tasks ($p_{\text{upper}} = .009$, $p_{\text{lower}} = .056$) were
572 significant. Overall, these results indicate dissimilar effects of motor tempo over the
573 motor region. A oneway RM ANOVA (Task Complexity [simple, moderate, complex])
574 was also computed but found to be nonsignificant ($p = .966$).

575 The RM ANOVA performed on the prefrontal channels showed a significant
576 main effect of motor tempo, $F(2, 30) = 6.11$, $p = .006$, $\eta_p^2 = .29$, with a larger $\bar{\Delta}_{\text{HbO}_2}$
577 in the 500 ms ISI ($M = 5.81$, $SD = 5.23$) than in the 1200 ms conditions ($M = 2.83$, SD
578 $= 5.14$, $d_z = 0.57$). Note that the effect size of the contrast was larger than the required
579 SESOI, which indicated that the effect was sufficiently strong to be considered

580 meaningful. The TOST procedure computed on the change score between the simple
581 and moderate tasks showed that both t tests were significant, $t_{\text{upper}}(15) = -2.97$, $p =$
582 $.005$, $t_{\text{lower}}(15) = 1.97$, $p = .034$. The same effects were observed between the simple and
583 complex tasks, $t_{\text{upper}}(15) = -2.64$, $p = .011$, $t_{\text{lower}}(15) = 1.82$, $p = .047$, and between the
584 moderate and complex tasks, $t_{\text{upper}}(15) = -2.38$, $p = .017$, $t_{\text{lower}}(15) = 2.08$, $p = .030$.
585 Overall, these results confirmed similar effects of motor tempo over the prefrontal
586 region, regardless of level of task complexity.

587

4. Discussion

588 The main purpose of the present study was to investigate frontal brain activity
589 under conditions of different speeds of motor execution. Three forms of upper-limb
590 movement were used as sensorimotor-synchronization tasks and performed at fast (i.e.,
591 300 ms), natural (i.e., 500 ms), and slow paces (i.e., 1200 ms). H_1 was not supported as
592 performing the tasks at spontaneous motor tempo did not yield less prefrontal and
593 motor activation than moving faster or slower. Action production at fast tempi led to
594 greater motor oxygenation compared to action production at slow tempi, which
595 replicated the previously-reported effect of larger increases in HbO₂ over the motor
596 cortex when a movement is executed at a fast pace (Kuboyama et al., 2004; Kuboyama
597 et al., 2005). However, moving at slow tempi did not lead to greater increases in
598 cerebral oxygenation over the prefrontal lobe when compared to the faster tempo.
599 Accordingly, H_2 is partially verified. Equivalence tests on task complexity were
600 significant for the two finger-tapping tasks only, and not for the continuous-drawing
601 task. Hence, H_3 was also only partially verified.

602 4.1 Cerebral Responses

603 Collectively, the present findings demonstrated the ability of f NIRS to dissociate
604 the involvement of different cognitive mechanisms as a function of task constraints. The
605 first important result is that the motor areas were activated to a greater degree when
606 producing actions at fast vs. slow tempi. In addition, TOST tests and descriptive data
607 confirmed that this pattern of results was potentiated in the complex task (i.e., circle
608 drawing; see Table 2). These findings are congruent with the *dynamic systems* approach

609 of motor timing, in which behavior is described as “the emergent product of a
610 self-organizing, multicomponent system evolving over time” (Perone & Simmering,
611 2017, p. 44). Indeed, behavioral studies have reported that the production of fast
612 movements is dependent on dynamic processes (Huys et al., 2008). In this respect, the
613 temporal organization of movements performed at 300 ms of ISI would emerge from the
614 regularities of body-dynamics (e.g., mass, length, velocity; Zelaznik et al., 2002). Hence,
615 there would be less cognitive control applied upon motor execution (Lemoine, 2007).
616 The findings of the present study extend the behavioral literature by providing evidence
617 that fast movement production is underpinned predominantly by central and
618 non-reflective motor processes.

619 The second important result is that performing a task at a slow pace did not
620 induce larger prefrontal hemodynamic responses when compared to performing at a fast
621 pace. Explanation for this unexpected finding lies with a measurement issue. Being
622 limited to 47 channels by our *f*NIRS system, we were not able to optimally cover the
623 prefrontal areas of the brain: A unique row of channels is accounted for on the
624 dorsolateral cortex. Therefore, it is possible that the ability to modulate motor tempo
625 according to environmental constraints is underpinned by cognitive functions that
626 might be pinpointed further forward in the brain.

627 By way of illustration, the medial prefrontal cortex has been proposed to control
628 the adaptive responses to context, location, and events (Di Pellegrino et al., 2007;
629 Euston et al., 2012), and could play a central role in performing a motor task at a slow
630 tempo. However, it would not have been recorded with the current *f*NIRS measurement
631 configuration. Even further frontal is the orbitofrontal cortex, which is implicated in
632 response inhibition (Evans et al., 2004; Horn et al., 2003). **In futures studies, there will**
633 **be** a clear need for more accurate contrasts of the activation loci evident across different
634 prefrontal areas. This will facilitate delineation of the frontal-cognitive processes that
635 underlie the ability to execute slow movements.

636 4.2 Spontaneous Motor Tempo

637 It is notable that motor timing at the spontaneous motor tempo led to greater
638 prefrontal activation. It could be that the recorded activation does not originate from
639 the dorsolateral cortex but from the supplementary motor area (SMA), which is located
640 close to the recorded channels. Using the *fOLD* toolbox (*fNIRS Optodes' Location*
641 *Decider*; Morais et al., 2018), we found that the recorded prefrontal activation had a
642 ~25% likelihood of having originated from the SMA. Relative to other neuroimaging
643 techniques (e.g., EEG), the *fNIRS* spatial resolution is quite good; nonetheless, the
644 measured activity is localized within the brain with an error of ~1 cm (Herold et al.,
645 2018). Therefore, the *fNIRS* technique may not afford sufficient fidelity to distinguish
646 dorsolateral prefrontal cortex activity from SMA activity.

647 Macar et al. (2006) proposed that, as part of the striato-cortical pathway, the
648 SMA plays a key role in time processing. In previous studies with *fMRI*, the pre-SMA
649 was found to be more activated when participants were directed to selectively attend to
650 time in perceptual-timing tasks (Coull, 2004; Coull et al., 2004). It is noteworthy that
651 the SMA was more involved for tempi close to spontaneous pace (i.e., 540 ms ISI) than
652 for slower tempi (i.e., 1080 ms ISI; Coull et al., 2012). There is similarity with the
653 present findings, which show significantly greater prefrontal activation in spontaneous
654 vs. slow-pace movement using analogous time intervals. In addition, patients with SMA
655 lesions have been reported to be impaired in rhythm-reproduction tasks in the absence
656 of auditory cues; nonetheless, they were perfectly able to produce rhythms when
657 auditory pacing was provided (Halsband et al., 1993). Accordingly, the SMA may be
658 more strenuously involved in internally-generated movements rather than in the
659 external guidance of timed movements (Rao et al., 1997). The increase of prefrontal
660 activation identified in the present study was occasioned by motor execution at a
661 spontaneous pace (i.e., the instinctive speed associated with self-initiated action). As
662 scientific knowledge stands, the cerebral correlates of motor production at a
663 spontaneous motor tempo are unclear. A plausible hypothesis emanating from the
664 present findings is that the SMA, and more specifically the pre-SMA, which has

665 projections to and from the prefrontal cortex (Kim et al., 2010), serves a pivotal role in
666 motor timing at (close-to-) spontaneous pace.

667 **4.3 Behavioral Outcome**

668 An original contribution of the present study concerns the three forms of
669 upper-limb movement that were used to control for motor complexity. The behavioral
670 results indicated that participants were less accurate in their time-interval production
671 when they performed the complex (i.e., circle-drawing task) vs. the easier tasks (i.e.,
672 finger-tapping and pointing tasks). The same pattern of results was found using *fNIRS*:
673 Identical effects of externally-paced tempo were observed for both the prefrontal and
674 motor areas between the simple and moderate tasks, but not between these tasks and
675 their complex counterpart. Accordingly, it seems that the performance of a timing task
676 is more laborious in continuous motion than in discrete actions.

677 Discrete actions are characterized by a recognizable beginning and end; thus,
678 they are much easier to synchronize with external events than continuous movements,
679 for which there is no recognizable beginning and end. In the present study, motor
680 activation could have been more salient when motor-timing control was challenging.
681 Interestingly, the complementary analysis (performed on the first peak of hemodynamic
682 activation) showed that an externally-paced tempo elicited similar effects regardless of
683 motor complexity in the prefrontal cortex. Conversely, the three equivalence tests failed
684 to reach significance in terms of the activation of motor areas. This finding suggests
685 that the three upper-limb movements required different planning and execution
686 strategies, but similar degrees of cognitive control for performance outcome.

687 **4.4 Strengths and Limitations**

688 The combination of *fNIRS* measurement with physiological indices has been
689 advocated in recent years and referred to as *systemic-physiology-augmented fNIRS*
690 (SPA-*fNIRS*; Scholkmann et al., 2017). The *fNIRS* technique enables the researcher to
691 draw inferences about neural activity through the assessment of cerebral blood
692 oxygenation. However, given that cardiac contractions contribute significantly to
693 cerebral oxygen supply, the frequency of these contractions must be identified in the

694 *f*NIRS signal of interest. Without such identification, the recorded signal might only
695 contains non-physiological fluctuations. In the present study, the validity of the
696 recorded *f*NIRS signal was verified through detailed observation of the relevant
697 physiological information derived from the *f*NIRS channels (i.e., HR and respiratory
698 frequency; see Figure 6). Collectively, the preprocessing data confirmed that the
699 application of *f*NIRS to motor paradigms is a scientifically legitimate endeavor.
700 Furthermore, we illustrated the importance of using physiological measurements to
701 identify and select the channels of interest. Therefore, it is evident that SPA-*f*NIRS
702 should be used in a systematic manner to verify that *f*NIRS data are sound, even in
703 experimental paradigms that do not involve movement-based tasks.

704 The methodological advancement evident in the present study entails a rigorous
705 procedure for the acquisition and processing of *f*NIRS data in the realm of whole-body
706 movement. First, a 3D reconstruction of the headset position on the participant's head
707 was used. This control is of paramount importance, as it enables the researcher to
708 ascertain the precise location of the recorded *f*NIRS signal throughout an experimental
709 session. In the current study, no *f*NIRS headset shifts were detected (on average, < 1%
710 of variation during the experimental session), even in tasks requiring moving through
711 space (e.g., the circle-drawing trials). Second, channel selection was undertaken to
712 ascertain whether cardiac frequency was visible in the *f*NIRS signals (Pinti et al., 2019).
713 Through this preprocessing method, only those channels with meaningful inputs were
714 kept in the regions of interest. Finally, a hybrid filter technique that was applied proved
715 effective in removing instrumental noise, motion-related artefacts, and physiological
716 oscillations (for a review of noise source in *f*NIRS signals, see Herold et al., 2018)
717 without overfiltering the signal, which seems to be a common phenomenon in the NIRS
718 literature.

719 In terms of limitations of the present study, the three types of upper-limb
720 movements that were chosen are simple laboratory-based tasks that have limited
721 ecological validity. In addition, it is possible that the natural-pace condition did not
722 best reflect the spontaneous motor tempo of a few participants. A condition developed

723 from prior measurement of each participant's spontaneous motor tempo could have
724 enhanced internal validity somewhat. The decision to select only participants with very
725 short hair (< 1 cm) is also acknowledged as a minor limitation. Given that only male
726 participants were recruited, we cannot readily generalize the findings to both sexes.

727 4.5 Future Directions

728 The present work serves to illustrate the technical challenges related to using
729 whole-brain *f*NIRS in movement paradigms. Nonetheless, a few recent articles providing
730 recommendations for *f*NIRS application are beginning to emerge in the scientific
731 literature (e.g., Herold et al., 2018; Perrey, 2014; Pinti et al., 2019). It is hoped that
732 researchers will take up the gauntlet of investigating cognitive processes underlying time
733 production and use realistic, whole-body movements in so doing. Such explorations will
734 represent a meaningful contribution to the knowledge base of cognitive neuroscience by
735 providing a broader picture of how the brain modulates motor timing.

736 Future research might also address the role of the brain's functional connectivity
737 in the adaptation of motor timing (see Vergotte et al., 2018; Vergotte et al., 2017). The
738 assessment of *f*NIRS connectivity between the prefrontal cortex and motor areas holds
739 potential to provide valuable insights on the cerebral dynamics underlying time
740 production. This form of rich detail is obfuscated when researchers focus solely upon
741 the activation pattern of one or two regions of interest.

742 From a methodological point of view, future research will need to tackle the
743 dissociation of prefrontal from SMA activations. With this aim in mind, it will be
744 appropriate to take anatomical specificity into account through tailoring the placement
745 of *f*NIRS channels to the brain morphology of each participant; this *neuronavigational*
746 *approach* will substantially increase the accurate identification of the brain areas of
747 interest (Herold et al., 2018). Close attention will also need to be given to the choice of
748 experimental motor tasks, as different brain patterns can be observed as a function of
749 the discrete vs. continuous dimension of motor skill execution. Researchers might use
750 naturalistic movements that mirror those used in everyday life, such as walking or
751 cycling.

752 4.6 Conclusions and Recommendations

753 When examined collectively, the present findings indicate that motor tasks
754 performed either at a fast or slow tempo will result in differences in brain activation.
755 *f*NIRS can be used to gain a fuller understanding of the brain dynamics involved in the
756 modulation of motor tempo. Fast pacing relies on greater activity of the motor areas
757 whereas moving at close-to-spontaneous pace places a heavier load on posterior
758 prefrontal processes. These findings are consistent with the notion that two timing
759 modes exist (see Huys et al., 2008; Madison & Delignieres, 2009); they confirm that the
760 execution of fast movements (i.e., faster than the spontaneous motor tempo) depend on
761 dynamic systems from which bodily movements emerge (Zelaznik et al., 2002). The
762 effects of spontaneous motor pacing on prefrontal brain activity are possibly the result
763 of the SMA involvement for motor execution at natural pace. With *f*NIRS technology,
764 the scientific community has a means by which to unravel the mystery surrounding how
765 the brain controls time production.

766

References

- 767 Abiru, M., Sakai, H., Sawada, Y., & Yamane, H. (2016). The effect of the challenging
768 two handed rhythm tapping task to DLPFC activation. *Asian Journal of*
769 *Occupational Therapy, 12*(1), 75–83. <https://doi.org/10.11596/asiajot.12.75>
- 770 Attwell, D., Buchan, A. M., Charpak, S., Lauritzen, M., MacVicar, B. A., &
771 Newman, E. A. (2010). Glial and neuronal control of brain blood flow. *Nature,*
772 *468*(7321), 232–243. <https://doi.org/10.1038/nature09613>
- 773 Baker, W. B., Parthasarathy, A. B., Busch, D. R., Mesquita, R. C., Greenberg, J. H., &
774 Yodh, A. (2014). Modified Beer-Lambert law for blood flow. *Biomedical Optics*
775 *Express, 5*(11), 4053–4075. <https://doi.org/10.1364/BOE.5.004053>
- 776 Bareš, M., Apps, R., Avanzino, L., Breska, A., D'Angelo, E., Filip, P., Gerwig, M.,
777 Ivry, R. B., Lawrenson, C. L., Louis, E. D., Lusk, N. A., Manto, M.,
778 Meck, W. H., Mitoma, H., & Petter, E. A. (2019). Consensus paper: Decoding
779 the contributions of the cerebellum as a time machine. From neurons to clinical
780 applications. *The Cerebellum, 18*(2), 266–286.
781 <https://doi.org/10.1007/s12311-018-0979-5>
- 782 Blampain, J., Ott, L., & Delevoeye-Turrell, Y. N. (2018). Seeing action simulation as it
783 unfolds: The implicit effects of action scenes on muscle contraction evidenced
784 through the use of a grip-force sensor. *Neuropsychologia, 114*, 231–242.
785 <https://doi.org/10.1016/j.neuropsychologia.2018.04.026>
- 786 Bobin-Bègue, A., Provasi, J., Marks, A., & Pouthas, V. (2006). Influence of auditory
787 tempo on the endogenous rhythm of non-nutritive sucking. *European Review of*
788 *Applied Psychology, 56*(4), 239–245. <https://doi.org/10.1016/j.erap.2005.09.006>
- 789 Bobin-Bègue, A., & Provasi, J. (2008). Régulation rythmique avant 4 ans : Effet d'un
790 tempo auditif sur le tempo moteur [Rhythmic regulation before 4 years: Effect of
791 an auditory tempo on the motor tempo]. *L'Année Psychologique, 108*, 631–658.
792 <https://frama.link/78H2hzbzN>

- 793 Bove, M., Tacchino, A., Pelosin, E., Moisello, C., Abbruzzese, G., & Ghilardi, M. F.
794 (2009). Spontaneous movement tempo is influenced by observation of rhythmical
795 actions. *Brain Research Bulletin*, *80*(3), 122–127.
796 <https://doi.org/10.1016/j.brainresbull.2009.04.008>
- 797 Bryant, G. A., & Barrett, H. C. (2007). Recognizing intentions in infant-directed
798 speech: Evidence for universals. *Psychological Science*, *18*(8), 746–751.
799 <https://doi.org/10.1111/j.1467-9280.2007.01970.x>
- 800 Buhusi, C. V., & Meck, W. H. (2005). What makes us tick? Functional and neural
801 mechanisms of interval timing. *Nature Reviews Neuroscience*, *6*(10), 755–765.
802 <https://doi.org/10.1038/nrn1764>
- 803 Campbell, H., & Lakens, D. (2020). Can we disregard the whole model? Omnibus
804 non-inferiority testing for R^2 in multivariable linear regression and η^2 in
805 ANOVA. *British Journal of Mathematical and Statistical Psychology*, Advance
806 online publication. <https://doi.org/10.1111/bmsp.12201>
- 807 Coull, J. T. (2004). fMRI studies of temporal attention: Allocating attention within, or
808 towards, time. *Cognitive Brain Research*, *21*(2), 216–226.
809 <https://doi.org/10.1016/j.cogbrainres.2004.02.011>
- 810 Coull, J. T., Hwang, H. J., Leyton, M., & Dagher, A. (2012). Dopamine precursor
811 depletion impairs timing in healthy volunteers by attenuating activity in
812 putamen and supplementary motor area. *Journal of Neuroscience*, *32*(47),
813 16704–16715. <https://doi.org/10.1523/JNEUROSCI.1258-12.2012>
- 814 Coull, J. T., Vidal, F., Nazarian, B., & Macar, F. (2004). Functional anatomy of the
815 attentional modulation of time estimation. *Science*, *303*(5663), 1506–1508.
816 <https://doi.org/10.1126/science.1091573>
- 817 Cribbie, R. A., Ragoonanan, C., & Counsell, A. (2016). Testing for negligible
818 interaction: A coherent and robust approach. *British Journal of Mathematical
819 and Statistical Psychology*, *69*(2), 159–174. <https://doi.org/10.1111/bmsp.12066>

- 820 Derosière, G., Alexandre, F., Bourdillon, N., Mandrick, K., Ward, T. E., & Perrey, S.
821 (2014). Similar scaling of contralateral and ipsilateral cortical responses during
822 graded unimanual force generation. *NeuroImage*, *85*, 471–477.
823 <https://doi.org/10.1016/j.neuroimage.2013.02.006>
- 824 Di Pellegrino, G., Ciaramelli, E., & Làdavas, E. (2007). The regulation of cognitive
825 control following rostral anterior cingulate cortex lesion in humans. *Journal of*
826 *Cognitive Neuroscience*, *19*(2), 275–286.
827 <https://doi.org/10.1162/jocn.2007.19.2.275>
- 828 Dione, M., & Delevoeye-Turrell, Y. (2015). Testing the co-existence of two timing
829 strategies for motor control in a unique task: The synchronisation
830 spatial-tapping task. *Human Movement Science*, *43*, 45–60.
831 <https://doi.org/10.1016/j.humov.2015.06.009>
- 832 Drake, C., & Baruch, C. (1995). De la mesure de la sensibilité temporelle aux modèles
833 d'organisation temporelle : Hypothèses et données sur l'acquisition des capacités
834 temporelles auditives [From measurement of temporal sensitivity to temporal
835 organization models: Hypotheses and data on the acquisition of temporal
836 auditory abilities]. *L'année Psychologique*, *95*(4), 555–569.
837 <https://doi.org/10.3406/psy.1995.28855>
- 838 Drenckhahn, C., Koch, S. P., Dümmler, J., Kohl-Bareis, M., Steinbrink, J., &
839 Dreier, J. P. (2015). A validation study of the use of near-infrared spectroscopy
840 imaging in primary and secondary motor areas of the human brain. *Epilepsy &*
841 *Behavior*, *49*, 118–125. <https://doi.org/10.1016/j.yebeh.2015.04.006>
- 842 Droit-Volet, S., & Wearden, J. (2003). Les modèles d'horloge interne en psychologie du
843 temps [Internal clock models in the psychology of time]. *L'année Psychologique*,
844 *103*(4), 617–654. <https://doi.org/10.3406/psy.2003.29656>
- 845 Euston, D. R., Gruber, A. J., & McNaughton, B. L. (2012). The role of medial
846 prefrontal cortex in memory and decision making. *Neuron*, *76*(6), 1057–1070.
847 <https://doi.org/10.1016/j.neuron.2012.12.002>

- 848 Evans, D. W., Lewis, M. D., & Iobst, E. (2004). The role of the orbitofrontal cortex in
849 normally developing compulsive-like behaviors and obsessive-compulsive
850 disorder. *Brain and Cognition*, *55*(1), 220–234.
851 [https://doi.org/10.1016/S0278-2626\(03\)00274-4](https://doi.org/10.1016/S0278-2626(03)00274-4)
- 852 Fraisse, P. (1974). *Psychologie du rythme* [Psychology of the rhythm]. Presses
853 Universitaires de France.
- 854 Fraisse, P. (1982). Rhythm and tempo. In D. Deutsch (Ed.), *The psychology of music*
855 (pp. 149–180). Academic Press.
- 856 Fraisse, P., Chambron, H., & Oléron, G. (1954). Note sur la constance et l'évolution
857 génétique du tempo spontané moteur [The constancy and genetic evolution of
858 spontaneous motor rhythm]. *Enfance*, *7*(1), 25–34.
859 <https://doi.org/10.3406/enfan.1954.1311>
- 860 Gervain, J., Mehler, J., Werker, J. F., Nelson, C. A., Csibra, G., Lloyd-Fox, S.,
861 Shukla, M., & Aslin, R. N. (2011). Near-infrared spectroscopy: A report from the
862 McDonnell infant methodology consortium. *Developmental Cognitive*
863 *Neuroscience*, *1*(1), 22–46. <https://doi.org/10.1016/j.dcn.2010.07.004>
- 864 Grahn, J. A., & Brett, M. (2007). Rhythm and beat perception in motor areas of the
865 brain. *Journal of Cognitive Neuroscience*, *19*(5), 893–906.
866 <https://doi.org/10.1162/jocn.2007.19.5.893>
- 867 Gusnard, D. A., & Raichle, M. E. (2001). Searching for a baseline: Functional imaging
868 and the resting human brain. *Nature Reviews Neuroscience*, *2*(10), 685–694.
869 <https://doi.org/10.1038/35094500>
- 870 Halsband, U., Ito, N., Tanji, J., & Freund, H.-J. (1993). The role of premotor cortex
871 and the supplementary motor area in the temporal control of movement in man.
872 *Brain*, *116*(1), 243–266. <https://doi.org/10.1093/brain/116.1.243>
- 873 Harms, C., & Lakens, D. (2018). Making 'null effects' informative: Statistical techniques
874 and inferential frameworks. *Journal of Clinical and Translational Research*,
875 *3*(Suppl. 2), 382–393. <https://doi.org/10.18053/jctres.03.2017S2.007>

- 876 Herold, F., Wiegel, P., Scholkmann, F., & Müller, N. G. (2018). Applications of
877 functional near-infrared spectroscopy (fNIRS) neuroimaging in
878 exercise–cognition science: A systematic, methodology-focused review. *Journal of*
879 *Clinical Medicine*, 7(12), Article e466. <https://doi.org/10.3390/jcm7120466>
- 880 Hocke, L. M., Oni, I. K., Duszynski, C. C., Corrigan, A. V., Frederick, B. d., &
881 Dunn, J. F. (2018). Automated processing of fNIRS data: A visual guide to the
882 pitfalls and consequences. *Algorithms*, 11(5), Article e67.
883 <https://doi.org/10.3390/a11050067>
- 884 Holper, L., Biallas, M., & Wolf, M. (2009). Task complexity relates to activation of
885 cortical motor areas during uni-and bimanual performance: A functional NIRS
886 study. *NeuroImage*, 46(4), 1105–1113.
887 <https://doi.org/10.1016/j.neuroimage.2009.03.027>
- 888 Homan, R. W., Herman, J., & Purdy, P. (1987). Cerebral location of international
889 10–20 system electrode placement. *Electroencephalography and Clinical*
890 *Neurophysiology*, 66(4), 376–382. [https://doi.org/10.1016/0013-4694\(87\)90206-9](https://doi.org/10.1016/0013-4694(87)90206-9)
- 891 Horn, N., Dolan, M., Elliott, R., Deakin, J. F., & Woodruff, P. (2003). Response
892 inhibition and impulsivity: An fMRI study. *Neuropsychologia*, 41(14),
893 1959–1966. [https://doi.org/10.1016/S0028-3932\(03\)00077-0](https://doi.org/10.1016/S0028-3932(03)00077-0)
- 894 Huys, R., Studenka, B. E., Rheaume, N. L., Zelaznik, H. N., & Jirsa, V. K. (2008).
895 Distinct timing mechanisms produce discrete and continuous movements. *PLOS*
896 *Computational Biology*, 4, Article e1000061.
897 <https://doi.org/10.1371/journal.pcbi.1000061>
- 898 Ivry, R. B., & Spencer, R. M. (2004). The neural representation of time. *Current*
899 *Opinion in Neurobiology*, 14(2), 225–232.
900 <https://doi.org/10.1016/j.conb.2004.03.013>
- 901 Jahani, S., Setarehdan, S. K., Boas, D. A., & Yücel, M. A. (2018). Motion artifact
902 detection and correction in functional near-infrared spectroscopy: A new hybrid
903 method based on spline interpolation method and Savitzky–Golay filtering.
904 *Neurophotonics*, 5(1), 1–11. <https://doi.org/10.1117/1.NPh.5.1.015003>

- 905 Jasper, H. H. (1958). Report of the Committee on Methods of Clinical Examination in
906 Electroencephalography. *Electroencephalography and Clinical Neurophysiology*,
907 10, 370–375. [https://doi.org/10.1016/0013-4694\(58\)90053-1](https://doi.org/10.1016/0013-4694(58)90053-1)
- 908 Jongasma, M. L., Meeuwissen, E., Vos, P. G., & Maes, R. (2007). Rhythm perception:
909 Speeding up or slowing down affects different subcomponents of the ERP P3
910 complex. *Biological Psychology*, 75(3), 219–228.
911 <https://doi.org/10.1016/j.biopsycho.2007.02.003>
- 912 Keele, S. W., Pokorny, R. A., Corcos, D. M., & Ivry, R. (1985). Do perception and
913 motor production share common timing mechanisms: A correlational analysis.
914 *Acta Psychologica*, 60(2–3), 173–191.
915 [https://doi.org/10.1016/0001-6918\(85\)90054-X](https://doi.org/10.1016/0001-6918(85)90054-X)
- 916 Kim, J.-H., Lee, J.-M., Jo, H. J., Kim, S. H., Lee, J. H., Kim, S. T., Seo, S. W.,
917 Cox, R. W., Na, D. L., Kim, S. I., et al. (2010). Defining functional SMA and
918 pre-SMA subregions in human MFC using resting state *fMRI*: Functional
919 connectivity-based parcellation method. *NeuroImage*, 49(3), 2375–2386.
920 <https://doi.org/10.1016/j.neuroimage.2009.10.016>
- 921 Kuboyama, N., Nabetani, T., Shibuya, K.-i., Machida, K., & Ogaki, T. (2004). The
922 effect of maximal finger tapping on cerebral activation. *Journal of Physiological*
923 *Anthropology and Applied Human Science*, 23(4), 105–110.
924 <https://doi.org/10.2114/jpa.23.105>
- 925 Kuboyama, N., Nabetani, T., Shibuya, K., Machida, K., & Ogaki, T. (2005).
926 Relationship between cerebral activity and movement frequency of maximal
927 finger tapping. *Journal of Physiological Anthropology and Applied Human*
928 *Science*, 24(3), 201–208. <https://doi.org/10.2114/jpa.24.201>
- 929 Lakens, D. (2017). Equivalence tests: A practical primer for *t* tests, correlations, and
930 meta-analyses. *Social Psychological and Personality Science*, 8(4), 355–362.
931 <https://doi.org/10.1177/1948550617697177>

- 932 Lakens, D., Scheel, A. M., & Isager, P. M. (2018). Equivalence testing for psychological
933 research: A tutorial. *Advances in Methods and Practices in Psychological*
934 *Science*, 1(2), 259–269. <https://doi.org/10.1177/2515245918770963>
- 935 Leff, D. R., Orihuela-Espina, F., Elwell, C. E., Athanasiou, T., Delpy, D. T.,
936 Darzi, A. W., & Yang, G.-Z. (2011). Assessment of the cerebral cortex during
937 motor task behaviours in adults: A systematic review of functional near infrared
938 spectroscopy (fNIRS) studies. *NeuroImage*, 54(4), 2922–2936.
939 <https://doi.org/10.1016/j.neuroimage.2010.10.058>
- 940 Lemoine, L. (2007). *Implication des processus de timing évènementiels et émergents*
941 *dans la gestion des aspects temporels du mouvement* (Doctoral dissertation).
942 Montpellier 1.
- 943 León-Carrión, J., & León-Dominguez, U. (2012). Functional near-infrared spectroscopy
944 (fNIRS): Principles and neuroscientific applications. In P. Bright (Ed.),
945 *Neuroimaging-Methods* (pp. 47–74). InTech.
- 946 Lewkowicz, D., & Delevoye-Turrell, Y. (2016). Real-time motion capture toolbox
947 (RTMocap): An open-source code for recording 3-D motion kinematics to study
948 action–effect anticipations during motor and social interactions. *Behavior*
949 *Research Methods*, 48(1), 366–380. <https://doi.org/10.3758/s13428-015-0580-5>
- 950 Macar, F., Coull, J., & Vidal, F. (2006). The supplementary motor area in motor and
951 perceptual time processing: fMRI studies. *Cognitive Processing*, 7(2), 89–94.
952 <https://doi.org/10.1007/s10339-005-0025-7>
- 953 Madison, G., & Delignieres, D. (2009). Auditory feedback affects the long-range
954 correlation of isochronous serial interval production: Support for a closed-loop or
955 memory model of timing. *Experimental Brain Research*, 193(4), 519–527.
956 <https://doi.org/10.1007/s00221-008-1652-x>
- 957 Magistretti, P. J., Pellerin, L., Rothman, D. L., & Shulman, R. G. (1999). Energy on
958 demand. *Science*, 283(5401), 496–497.
959 <https://doi.org/10.1126/science.283.5401.496>

- 960 Mandrick, K. (2013). *Application de la spectroscopie proche infrarouge dans la*
961 *discrimination de la charge de travail* [Doctoral dissertation, Montpellier 1].
962 <https://tel.archives-ouvertes.fr/tel-00868844/>
- 963 Mandrick, K., Derosiere, G., Dray, G., Coulon, D., Micallef, J.-P., & Perrey, S. (2013).
964 Prefrontal cortex activity during motor tasks with additional mental load
965 requiring attentional demand: A near-infrared spectroscopy study. *Neuroscience*
966 *Research, 76*(3), 156–162. <https://doi.org/10.1016/j.neures.2013.04.006>
- 967 Mates, J., Müller, U., Radil, T., & Pöppel, E. (1994). Temporal integration in
968 sensorimotor synchronization. *Journal of Cognitive Neuroscience, 6*(4), 332–340.
969 <https://doi.org/10.1162/jocn.1994.6.4.332>
- 970 McAuley, J. D., Jones, M. R., Holub, S., Johnston, H. M., & Miller, N. S. (2006). The
971 time of our lives: Life span development of timing and event tracking. *Journal of*
972 *Experimental Psychology: General, 135*(3), 348–367.
973 <https://doi.org/10.1037/0096-3445.135.3.34>
- 974 McIntosh, M. A., Shahani, U., Boulton, R. G., & McCulloch, D. L. (2010). Absolute
975 quantification of oxygenated hemoglobin within the visual cortex with functional
976 near infrared spectroscopy (fNIRS). *Investigative Ophthalmology & Visual*
977 *Science, 51*(9), 4856–4860. <https://doi.org/10.1167/iovs.09-4940>
- 978 Micklewright, D., Gibson, A. S. C., Gladwell, V., & Al Salman, A. (2017). Development
979 and validity of the rating-of-fatigue scale. *Sports Medicine, 47*(11), 2375–2393.
980 <https://doi.org/10.1007/s40279-017-0711-5>
- 981 Miyai, I., Tanabe, H. C., Sase, I., Eda, H., Oda, I., Konishi, I., Tsunazawa, Y.,
982 Suzuki, T., Yanagida, T., & Kubota, K. (2001). Cortical mapping of gait in
983 humans: A near-infrared spectroscopic topography study. *NeuroImage, 14*(5),
984 1186–1192. <https://doi.org/10.1006/nimg.2001.0905>
- 985 Moelants, D. (2002). Preferred tempo reconsidered. In D. G. Nair, E. W. Large,
986 F. Steinberg, J. A. S. Kelso, K. Stevens, D. Burnham, & J. Renwick (Eds.),
987 *Proceedings of the 7th International Conference on Music Perception and*
988 *Cognition* (pp. 1–4). <https://frama.link/8EpG2BtE>

- 989 Molavi, B., & Dumont, G. A. (2012). Wavelet-based motion artifact removal for
990 functional near-infrared spectroscopy. *Physiological Measurement*, *33*(2),
991 259–270. <https://doi.org/10.1088/0967-3334/33/2/259>
- 992 Morais, G. A. Z., Balardin, J. B., & Sato, J. R. (2018). FNIRS optodes' location decider
993 (fOLD): A toolbox for probe arrangement guided by brain regions-of-interest.
994 *Scientific reports*, *8*(1), 1–11. <https://doi.org/10.1038/s41598-018-21716-z>
- 995 Obrig, H., Hirth, C., Junge-Hülsing, J. G., Döge, C., Wenzel, R., Wolf, T., Dirnagl, U.,
996 & Villringer, A. (1997). Length of resting period between stimulation cycles
997 modulates hemodynamic response to a motor stimulus. In I. R. Cohen,
998 A. Lajtha, J. D. Lambris, R. Paoletti, & N. Rezaei (Eds.), *Oxygen transport to*
999 *tissue XVIII* (pp. 471–480). Springer.
- 1000 Okamoto, M., Dan, H., Sakamoto, K., Takeo, K., Shimizu, K., Kohno, S., Oda, I.,
1001 Isobe, S., Suzuki, T., Kohyama, K., & Dan, I. (2004). Three-dimensional
1002 probabilistic anatomical cranio-cerebral correlation via the international 10–20
1003 system oriented for transcranial functional brain mapping. *NeuroImage*, *21*(1),
1004 99–111. <https://doi.org/10.1016/j.neuroimage.2003.08.026>
- 1005 Oldfield, R. C. (1971). The assessment and analysis of handedness: The Edinburgh
1006 inventory. *Neuropsychologia*, *9*(1), 97–113.
1007 <http://andersgade.dk/Readings/Oldfield1971.pdf>
- 1008 Orihuela-Espina, F., Leff, D. R., James, D. R., Darzi, A. W., & Yang, G.-Z. (2010).
1009 Quality control and assurance in functional near infrared spectroscopy (fNIRS)
1010 experimentation. *Physics in Medicine & Biology*, *55*(13), 3701.
1011 <https://doi.org/10.1088/0031-9155/55/13/009>
- 1012 Perone, S., & Simmering, V. R. (2017). Applications of dynamic systems theory to
1013 cognition and development: New frontiers. In J. B. Benson (Ed.), *Advances in*
1014 *child development and behavior* (pp. 43–80). Academic Press.
- 1015 Perrey, S. (2014). Possibilities for examining the neural control of gait in humans with
1016 fNIRS. *Frontiers in Physiology*, *5*, Article e204.
1017 <https://doi.org/10.3389/fphys.2014.00204>

- 1018 Pinti, P., Scholkmann, F., Hamilton, A., Burgess, P., & Tachtsidis, I. (2019). Current
1019 status and issues regarding pre-processing of *fnirs* neuroimaging data: An
1020 investigation of diverse signal filtering methods within a general linear model
1021 framework. *Frontiers in Human Neuroscience*, *12*, Article e505.
1022 <https://doi.org/10.3389/fnhum.2018.00505>
- 1023 Pringle, J., Roberts, C., Kohl, M., & Lekeux, P. (1999). Near infrared spectroscopy in
1024 large animals: Optical pathlength and influence of hair covering and epidermal
1025 pigmentation. *The Veterinary Journal*, *158*(1), 48–52.
1026 <https://doi.org/10.1053/tvj.1998.0306>
- 1027 Quaresima, V., & Ferrari, M. (2016). Functional near-infrared spectroscopy (*fNIRS*) for
1028 assessing cerebral cortex function during human behavior in natural/social
1029 situations: A concise review. *Organizational Research Methods*, *22*(1), 1–23.
1030 <https://doi.org/10.1177/1094428116658959>
- 1031 Rao, S. M., Harrington, D. L., Haaland, K. Y., Bobholz, J. A., Cox, R. W., &
1032 Binder, J. R. (1997). Distributed neural systems underlying the timing of
1033 movements. *Journal of Neuroscience*, *17*(14), 5528–5535.
1034 <https://doi.org/10.1523/JNEUROSCI.17-14-05528.1997>
- 1035 Repp, B. H. (2005). Sensorimotor synchronization: A review of the tapping literature.
1036 *Psychonomic Bulletin & Review*, *12*(6), 969–992.
1037 <https://doi.org/10.3758/BF03206433>
- 1038 Rubia, K., & Smith, A. (2004). The neural correlates of cognitive time management: A
1039 review. *Acta Neurobiologiae Experimentalis*, *64*(3), 329–340.
1040 <http://psycnet.apa.org/record/2004-18721-004>
- 1041 Sato, T., Ito, M., Suto, T., Kameyama, M., Suda, M., Yamagishi, Y., Ohshima, A.,
1042 Uehara, T., Fukuda, M., & Mikuni, M. (2007). Time courses of brain activation
1043 and their implications for function: A multichannel near-infrared spectroscopy
1044 study during finger tapping. *Neuroscience Research*, *58*(3), 297–304.
1045 <https://doi.org/10.1016/j.neures.2007.03.014>

- 1046 Schmidt, R. A., Lee, T. D., Winstein, C., Wulf, G., & Zelaznik, H. N. (1988). *Motor*
1047 *control and learning: A behavioral emphasis* (6th ed.). Human Kinetics.
- 1048 Scholkmann, F., Hafner, T., Metz, A. J., Wolf, M., & Wolf, U. (2017). Effect of
1049 short-term colored-light exposure on cerebral hemodynamics and oxygenation,
1050 and systemic physiological activity. *NeuroPhotonics*, 4(4), Article e045005.
1051 <https://doi.org/10.1117/1.NPh.4.4.045005>
- 1052 Scholkmann, F., Kleiser, S., Metz, A. J., Zimmermann, R., Pavia, J. M., Wolf, U., &
1053 Wolf, M. (2014). A review on continuous wave functional near-infrared
1054 spectroscopy and imaging instrumentation and methodology. *NeuroImage*, 85,
1055 6–27. <https://doi.org/10.1016/j.neuroimage.2013.05.004>
- 1056 Schubotz, R. I., Friederici, A. D., & von Cramon, D. Y. (2000). Time perception and
1057 motor timing: A common cortical and subcortical basis revealed by fMRI.
1058 *NeuroImage*, 11(1), 1–12. <https://doi.org/10.1006/nimg.1999.0514>
- 1059 Shadgan, B., Molavi, B., Reid, W. D., Dumont, G., & Macnab, A. J. (2010). Do radio
1060 frequencies of medical instruments common in the operating room interfere with
1061 near-infrared spectroscopy signals? In T. Vo-Dinh, W. S. Grundfest, &
1062 A. Mahadevan-Jansen (Eds.), *Advanced biomedical and clinical diagnostic*
1063 *systems VIII* (pp. 1–6). <https://doi.org/10.1117/12.842712>
- 1064 Simonsohn, U. (2015). Small telescopes: Detectability and the evaluation of replication
1065 results. *Psychological Science*, 26(5), 559–569.
1066 <https://doi.org/10.1177/0956797614567341>
- 1067 Strangman, G., Boas, D. A., & Sutton, J. P. (2002). Non-invasive neuroimaging using
1068 near-infrared light. *Biological Psychiatry*, 52(7), 679–693.
1069 [https://doi.org/10.1016/S0006-3223\(02\)01550-0](https://doi.org/10.1016/S0006-3223(02)01550-0)
- 1070 Tachtsidis, I., Elwell, C. E., Leung, T. S., Lee, C.-W., Smith, M., & Delpy, D. T. (2004).
1071 Investigation of cerebral haemodynamics by near-infrared spectroscopy in young
1072 healthy volunteers reveals posture-dependent spontaneous oscillations.
1073 *Physiological Measurement*, 25(2), 437–445.
1074 <https://doi.org/10.1088/0967-3334/25/2/003>

- 1075 Tachtsidis, I., & Scholkmann, F. (2016). False positives and false negatives in functional
1076 near-infrared spectroscopy: Issues, challenges, and the way forward.
1077 *Neurophotonics*, 3(3), Article e031405.
1078 <https://doi.org/10.1117/1.NPh.3.3.031405>
- 1079 Treisman, M. (1963). Temporal discrimination and the indifference interval:
1080 Implications for a model of the "internal clock". *Psychological Monographs:*
1081 *General and Applied*, 77(13), 1–31. <https://doi.org/10.1037/h0093864>
- 1082 Vergotte, G., Perrey, S., Muthuraman, M., Janaqi, S., & Torre, K. (2018). Concurrent
1083 changes of brain functional connectivity and motor variability when adapting to
1084 task constraints. *Frontiers in Physiology*, 9, Article e909.
1085 <https://doi.org/10.3389/fphys.2018.00909>
- 1086 Vergotte, G., Torre, K., Chirumamilla, V. C., Anwar, A. R., Groppa, S., Perrey, S., &
1087 Muthuraman, M. (2017). Dynamics of the human brain network revealed by
1088 time-frequency effective connectivity in fNIRS. *Biomedical Optics Express*,
1089 8(11), 5326–5341. <https://doi.org/10.1364/BOE.8.005326>
- 1090 Williams, B. R., Ponesse, J. S., Schachar, R. J., Logan, G. D., & Tannock, R. (1999).
1091 Development of inhibitory control across the life span. *Developmental*
1092 *Psychology*, 35(1), 205–213. <http://psycnet.apa.org/buy/1998-03083-016>
- 1093 Wilson, T. W., Kurz, M. J., & Arpin, D. J. (2014). Functional specialization within the
1094 supplementary motor area: A fNIRS study of bimanual coordination.
1095 *NeuroImage*, 85(1), 445–450. <https://doi.org/10.1016/j.neuroimage.2013.04.112>
- 1096 Zelaznik, H. N., Spencer, R., & Ivry, R. B. (2002). Dissociation of explicit and implicit
1097 timing in repetitive tapping and drawing movements. *Journal of Experimental*
1098 *Psychology: Human Perception and Performance*, 28(3), 575.
1099 <https://doi.org/10.1037/0096-1523.28.3.575>

Table 1*Estimated Required Sample Size and Critical Statistical Tests*

Hypotheses	Groups	Measurements	Planned analysis	Critical statistical tests	Required sample size	SESOI
H_1	9	2	RM MANOVA	Contrast 1: 500 ms vs. 300 ms Contrast 2: 500 ms vs. 1200 ms	15	.22
H_2	9	2	RM MANOVA	300 ms vs. 1200 ms Simple vs. moderate task	16	.22
H_3	9	2	TOST	Simple vs. complex task Moderate vs. complex task	16	.22

Note. Statistical power, planned analyses, and critical statistical tests for each research hypothesis. SESOI = smallest effect size of interest (d_z);

TOSTs = two one-sided t tests.

Table 2

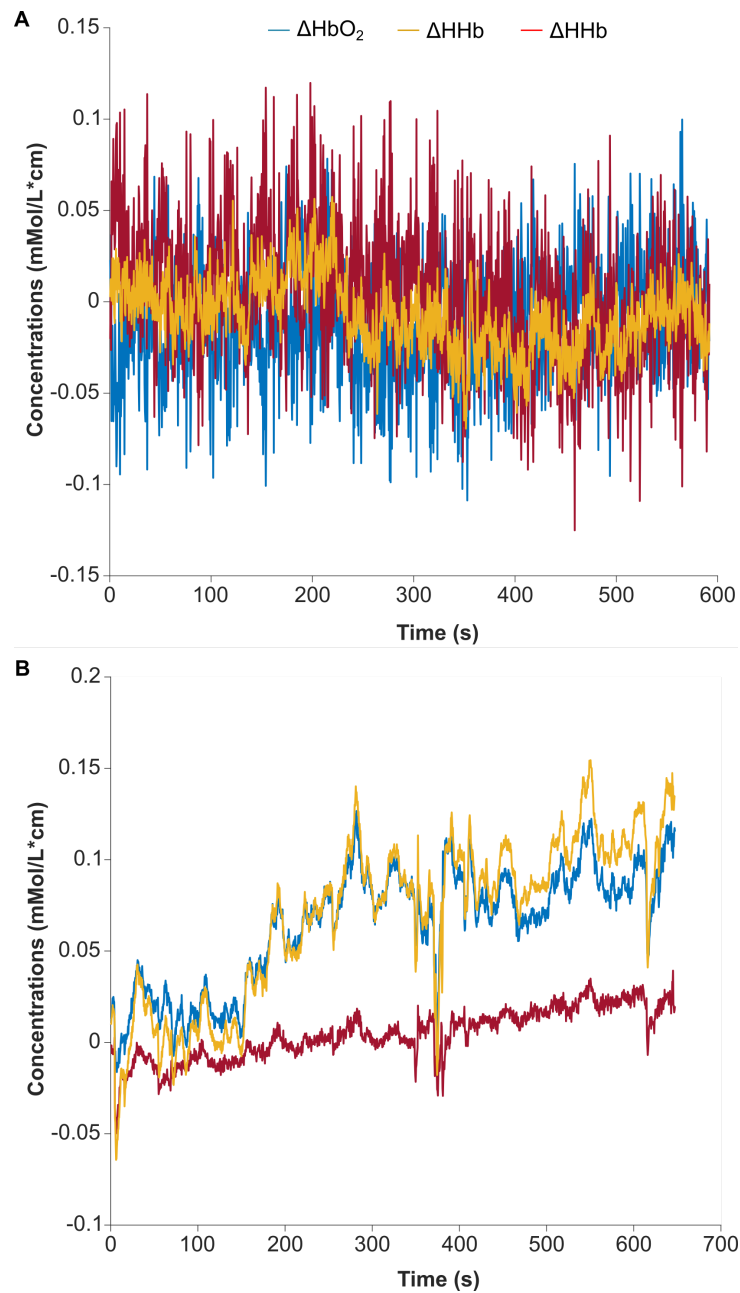
Oxyhemoglobin and Deoxyhemoglobin Change Scores Over the Motor and Prefrontal Regions of Interest

Regions of Interest	Oxyhemoglobin		Deoxyhemoglobin	
	<i>M</i>	<i>SD</i>	<i>M</i>	<i>SD</i>
Motor				
Simple	0.97	8.28	-0.15	1.99
Moderate	2.22	9.33	-0.36	2.15
Complex	5.54	7.65	0.46	3.09
Prefrontal				
Simple	0.51	6.61	-0.29	2.81
Moderate	0.75	8.06	0.04	1.50
Complex	2.45	8.24	0.40	3.45

Note. Means and standard deviations for oxyhemoglobin and deoxyhemoglobin change scores (i.e., $\bar{\Delta}_{\text{HbO}_2}$ 300 ms - $\bar{\Delta}_{\text{HbO}_2}$ 1200 ms) for each motor task. A positive value indicates higher activations for 300 ms vs. 1200 ms.

Figure 1

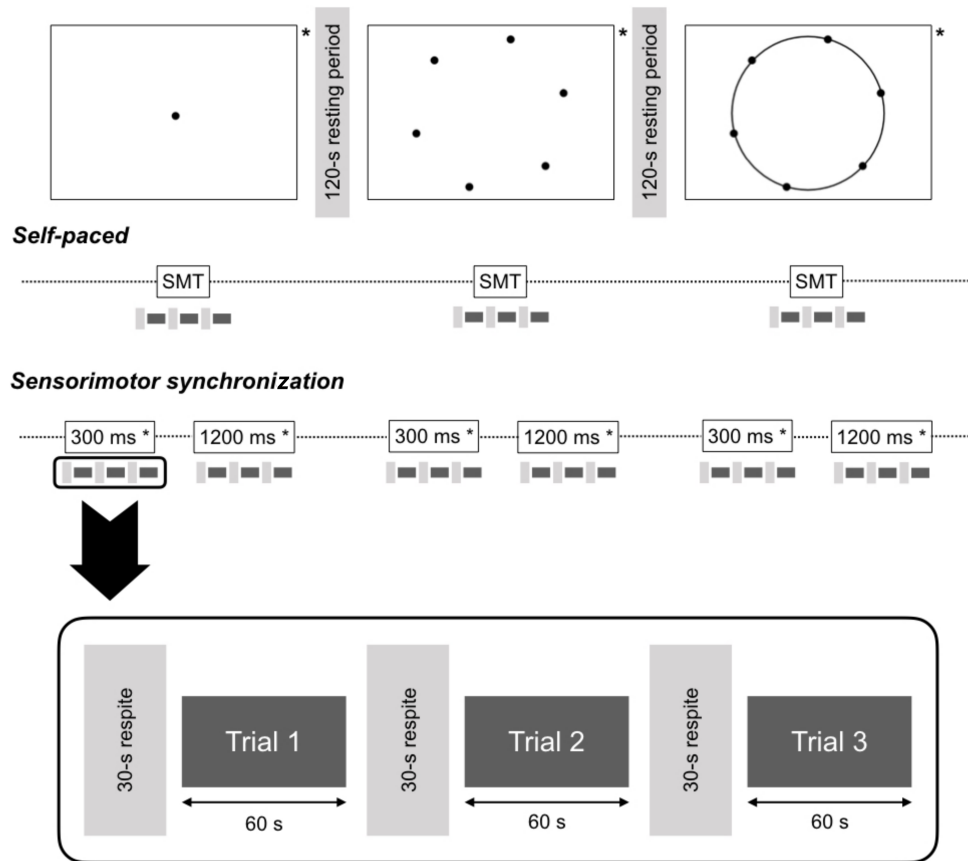
Raw fNIRS Data from a Participant With Hair vs. a Participant Without Hair



Note. Raw data for HbO_2 , HHb and HbT . Panel A: A typical participant with hair. Panel B: A typical participant without hair. These data were obtained from a pretest using two participants who performed the finger-tapping task synchronized to an auditory metronome at an interstimuli interval of 500 ms. HbO_2 = oxygenated hemoglobin; HHb = deoxygenated hemoglobin; HbT = total hemoglobin.

Figure 2

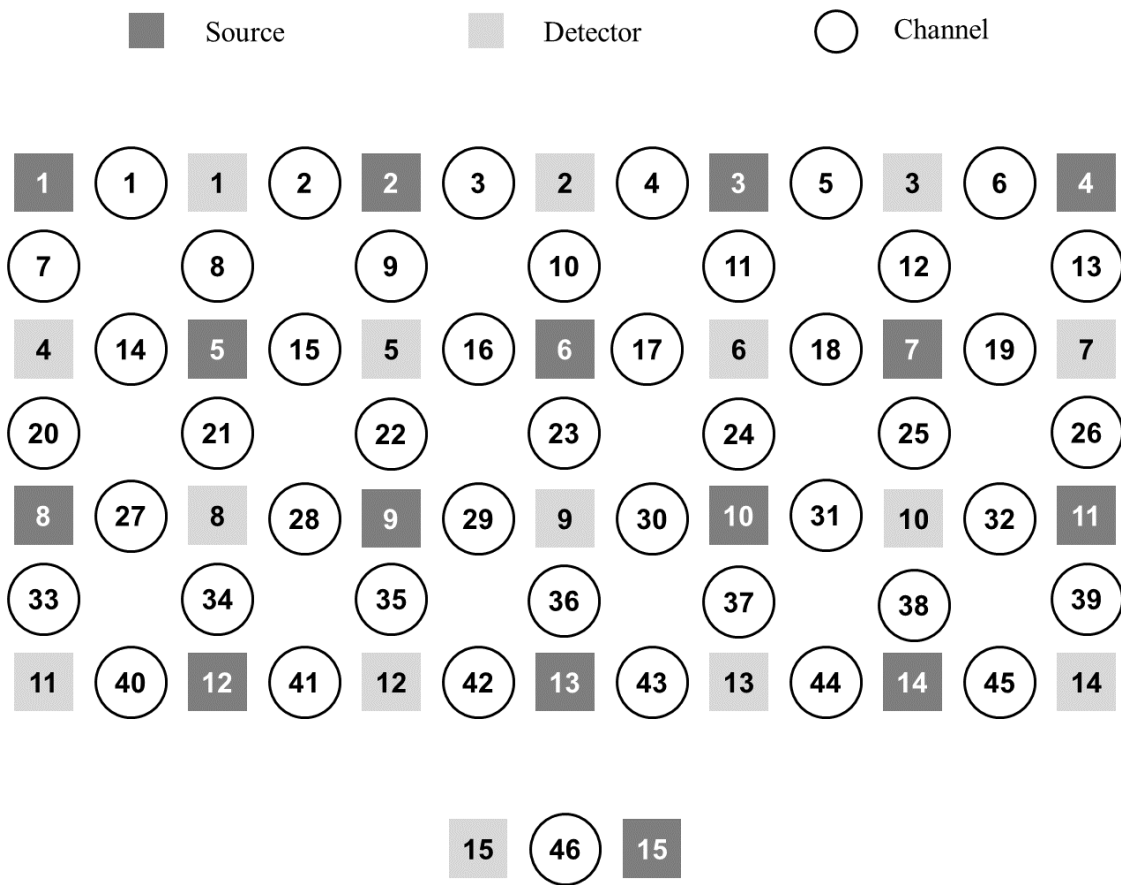
Diagrammatic Representation of the Experimental Design for the Sensorimotor Synchronization Conditions



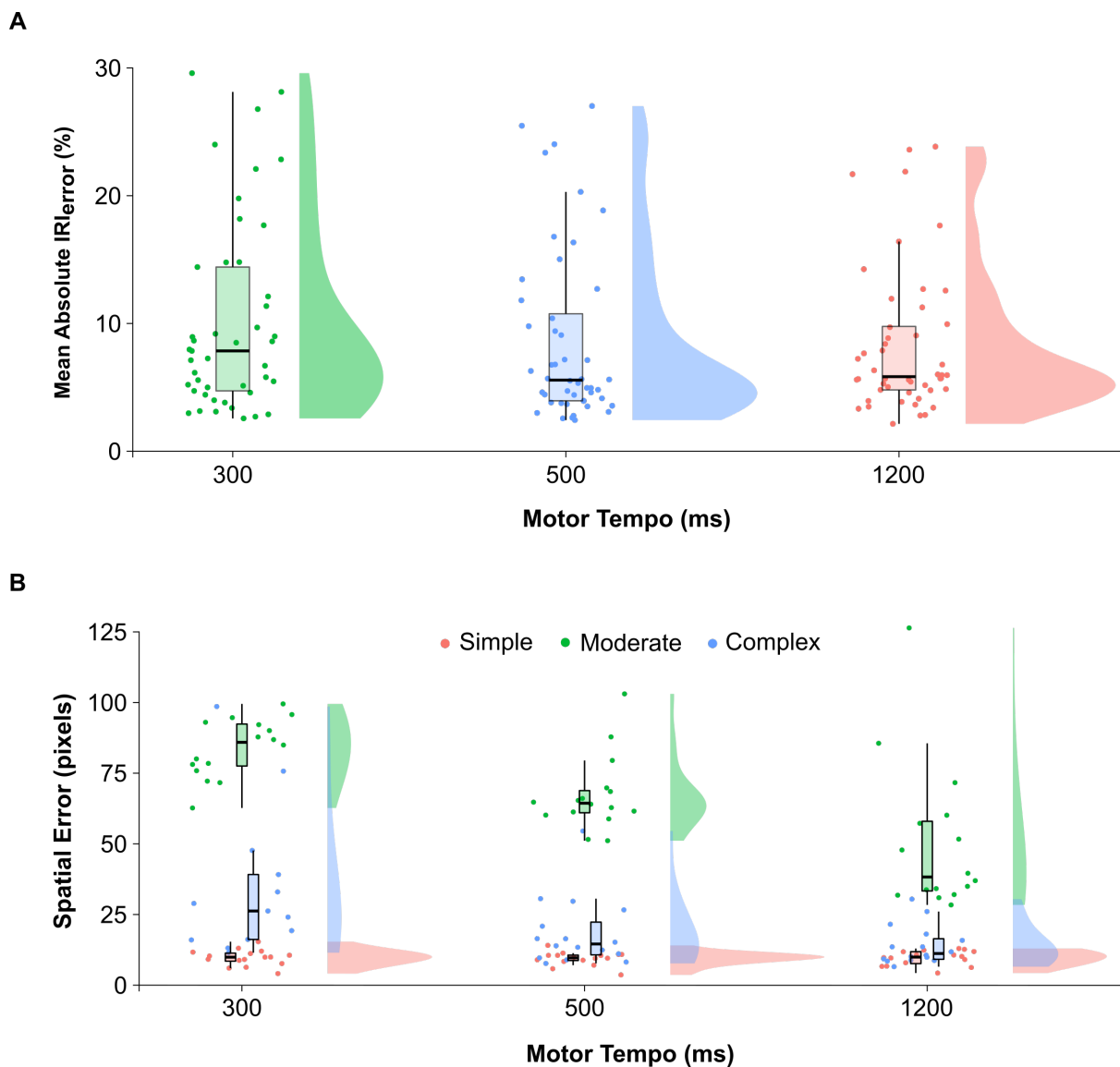
Note. SMT = spontaneous motor tempo; * = randomization.

Figure 3

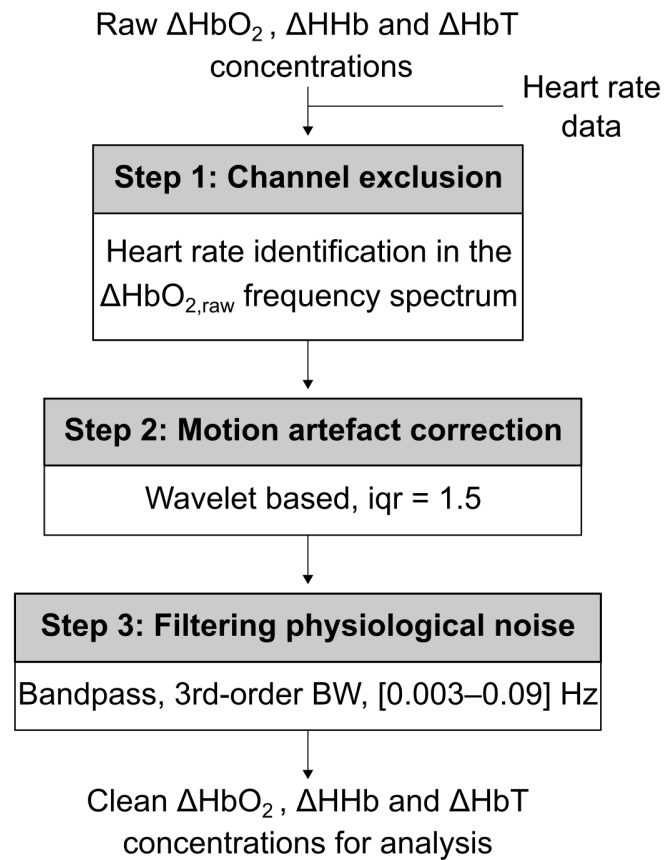
Diagrammatic Representation of the Sources, Detectors, and Channel Layout



Note. Adjacent sources and detectors were 3 cm apart.

Figure 4*Behavioral Results for Each Experimental Condition*

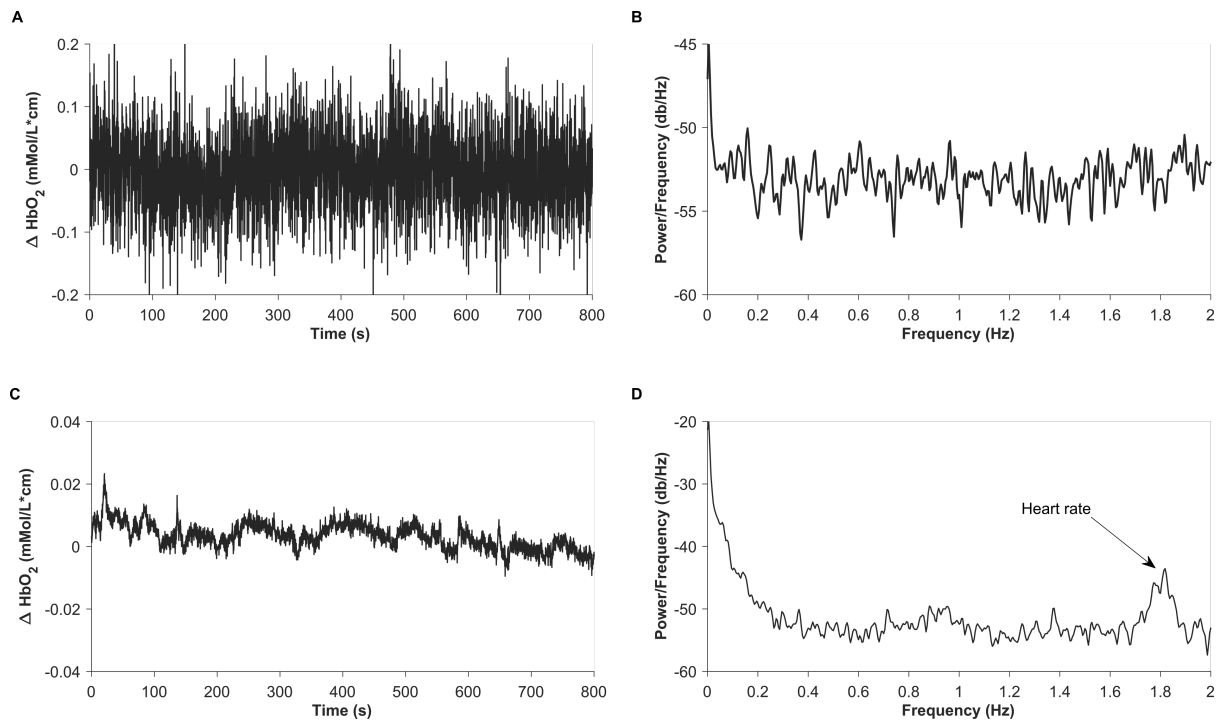
Note. Panel A: Mean IRI_{error}. Box plots and density distributions are displayed for each designated motor tempo. Each dot represents an individual participant. IRI = inter-response interval. Panel B: Mean spatial errors. Box plots and density distributions are displayed for each designated motor tempo and level of task complexity. Each dot represents an individual participant.

Figure 5*Preprocessing Pipeline of fNIRS Data*

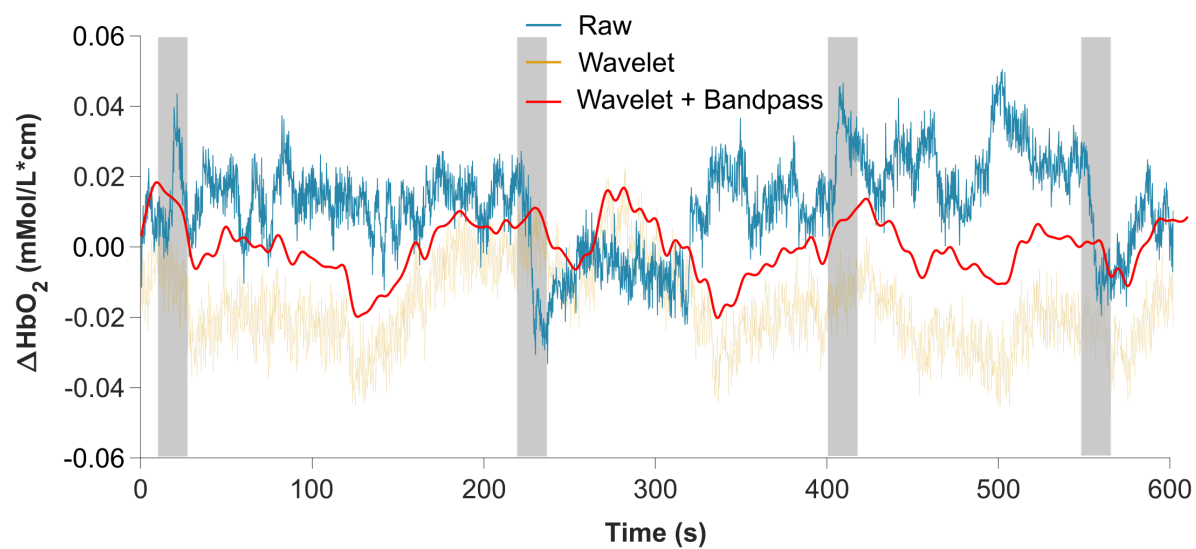
Note. HbO_2 = oxygenated-hemoglobin; HHb = deoxygenated-hemoglobin; iqr = interquartile range; BW = Butterworth filter.

Figure 6

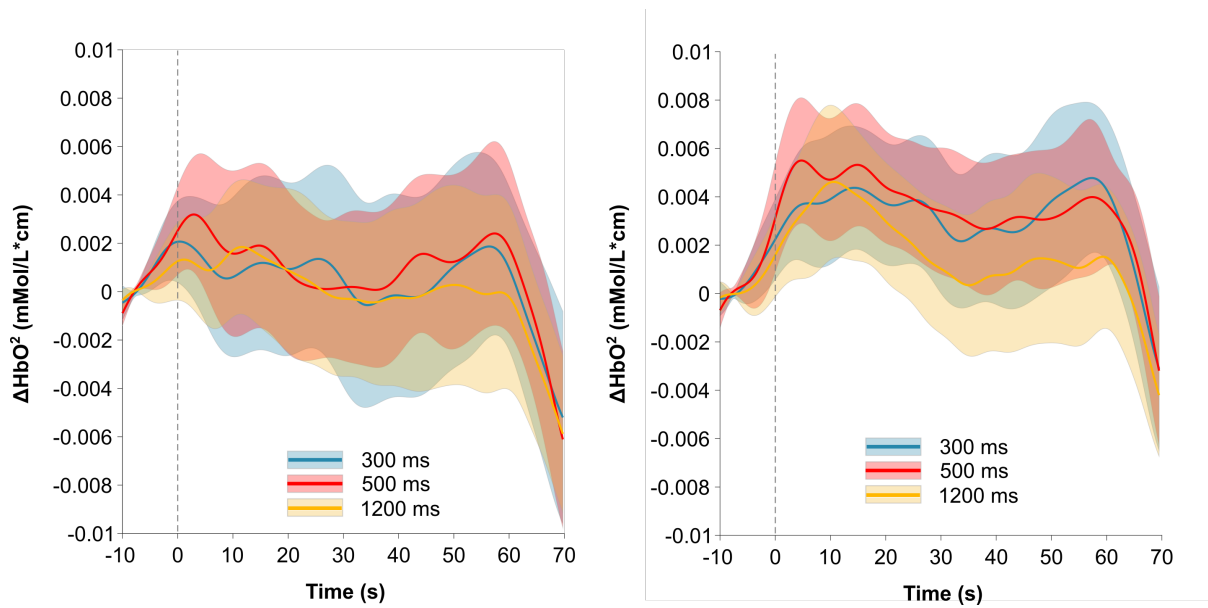
Raw Data and Power-Spectrum Density of Two Levels of Signal-to-Noise Ratio



Note. Samples of ΔHbO_2 recorded on channel 17 for two participants (left), and their respective power spectrum (right). Heart rate frequency was not identified in the power-spectrum density for a time-series with a poor signal-to-noise ratio (SNR; top right), but present with high SNR (bottom right).

Figure 7*Filtering of the fNIRS Signal*

Note. Example of the filtering of motion artefact (wavelet based, brown) and physiological noise (bandpass, red) from ΔHbO_2 data (channel 33, blue). Areas highlighted in gray represent motion-kind and baseline shift artefacts.

Figure 8*fNIRS Data for Each Experimental Condition*

Note. Panel A: Mean $\bar{\Delta}_{\text{HbO}_2}$ and $\bar{\Delta}_{\text{HHb}}$ for each motor tempo in the prefrontal channels. 95% confidence intervals are represented by the shaded area that surrounds each trace. Panel B: Mean $\bar{\Delta}_{\text{HbO}_2}$ and $\bar{\Delta}_{\text{HHb}}$ for each motor tempo in the motor channels. 95% confidence intervals are represented by the shaded area that surrounds each trace.